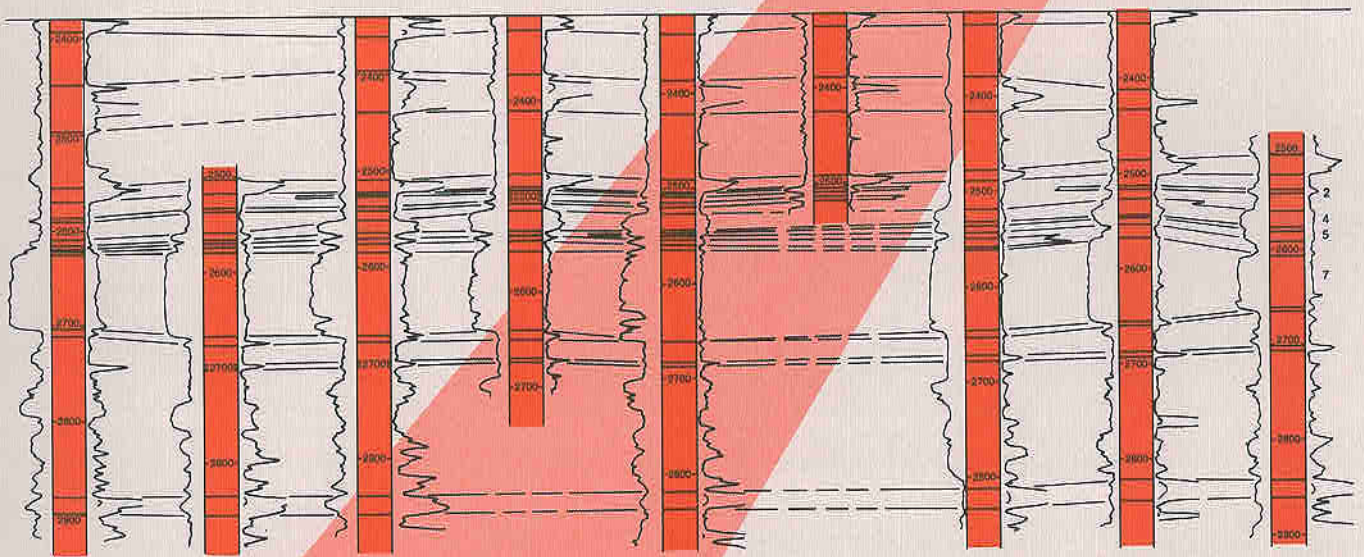


The Cypress Sandstone (Mississippian) Reservoir and Its Recovery Potential at Xenia East Oil Field, Clay County, Illinois

Jianzhong Xu and Bryan G. Huff



The Cypress Sandstone (Mississippian) Reservoir and Its Recovery Potential at Xenia East Oil Field, Clay County, Illinois

Jianzhong Xu and Bryan G. Huff

1995
Illinois Petroleum 147

ILLINOIS STATE GEOLOGICAL SURVEY
Jonathan H. Goodwin, Acting Chief
Natural Resources Building
615 E. Peabody Drive
Champaign, Illinois 61820-6964

Disclaimer

This report was prepared by the Illinois State Geological Survey (ISGS) for a project sponsored by the State of Illinois and the U.S. Department of Energy (USDOE). It presents reasonable interpretations of available scientific data. Any opinions, conclusions, or recommendations expressed in this report are those of the authors and do not necessarily reflect the views of the USDOE. Neither the ISGS, any member of the ISGS staff, the Illinois Department of Energy and Natural Resources, nor the USDOE assumes any liability with respect to the use, or for any damages resulting from the use, of information contained in this report. Use of a particular product does not constitute an endorsement by the ISGS or the USDOE.



CONTENTS

ABSTRACT	1
INTRODUCTION	3
Scope	3
Discovery and Development History	3
RESERVOIR AND TRAP CHARACTERISTICS	3
Stratigraphy	3
Reservoir Geometry	6
Trap Type	10
Reservoir Lithofacies	11
Depositional Environment	14
Diagenesis	23
Factors Controlling Reservoir Quality	25
CLASSIFICATION AND IDENTIFICATION OF PLAYS	30
PRODUCTION CHARACTERISTICS	32
Drilling and Completion Practices	32
Calculation of Reserves	33
Volumetrics: Monte Carlo technique	33
Volumetrics: planimeter measurements	36
Discussion of STOOIP and remaining mobile oil	36
DEVELOPMENT AND PRODUCTION STRATEGY	37
CONCLUSIONS	37
ACKNOWLEDGMENTS	38
REFERENCES	38
APPENDIXES	40
A Computer Program for the Monte Carlo Calculation	40
B Major Input and Output Data for the Monte Carlo Calculation	43
C Pickett Plot Data	45
D Reservoir Summary	46
TABLES	
1 Production and completion information for Cypress wells in the study area	5
2 Relative percentages of minerals in core samples, as determined by bulk volume (Keystone Oil Company, Campbell Heirs no. 3 well)	24
3 Planimeter measurements	36
FIGURES	
1 Locations and status of wells in Xenia East Field; also cross section lines A-A', B-B', C-C', D-D', and E-E'	2
2 Principal geologic structures in the center of the Illinois Basin	4
3 Generalized stratigraphic column of southern Illinois Basin	5
4 Production curves showing the decline that began the second year after the discovery of Xenia East Field	6
5 Thickness map of Cypress Sandstone at Xenia East Field	7
6 Total thickness of clean sandstone in the Cypress Sandstone at Xenia East Field	8
7 Typical E-logs showing the subdivision of sandstone units 1 to 7 of the Cypress Formation at Xenia East Field	9

8	Stratigraphic cross section A–A' showing the connection and distribution of sandstone units along a north–south line	10
9	Stratigraphic cross section B–B' showing the connection and distribution of sandstone units along an east–west line in the center of the field	12
10	Stratigraphic cross section C–C' showing the connection and distribution of sandstone units along an east–west line in the north part of the field	14
11	Structure map contoured on top of the Beech Creek Limestone ("Barlow")	15
12	Thickness map of clean unit 7 sandstone	16
13	Thickness map of clean unit 6 sandstone	17
14	Thickness map of clean unit 5 sandstone	18
15	Thickness map of clean unit 4 sandstone	19
16	Thickness map of clean unit 3 sandstone	20
17	Thickness map of unit 2 sandstone	21
18	Thickness map of clean unit 1 sandstone	22
19	Cross section D–D' showing the structural trap in the unit 4 sandstone	25
20	Thickness map of net pay zone unit 4 sandstone	26
21	Cross section E–E' showing the stratigraphic trap in unit 2 sandstone	30
22	A lithologic column and core analysis combined with an electric log; porosity (ϕ) and permeability (k) from the core analysis are plotted relative to depth	31
23	SEM/EDX spectrum of chlorite showing the percentages of elements	31
24	X-ray diffraction results showing the bulk mineral components of the reservoir sandstone; samples were taken from core plugs of the Campbell Heirs no. 3 well	32
25	Pay zone distribution function	34
26	Oil saturation distribution function	34
27	STOOIP distribution function	35
C-1	Pickett Plot showing the initial water–oil saturations of the reservoir	45

PLATES

1	Thin section of a sample from a depth of 2,544.5 feet in the Campbell Heirs no. 3 well; photomicrograph shows heavy mineral grain lag highlighting the crossbedding in very fine grained sandstone from unit 4	27
2	Close-up of the thin section in plate 1	27
3	Thin section of a sample from a depth of 2,535.5 feet in the Campbell Heirs no. 3 well; photomicrograph shows intergranular porosity types and quartz overgrowths	28
4	Partially dissolved plagioclase feldspar in the bottom center of the photomicrograph of a thin section of a sample from a depth of 2,542.5 feet in the Campbell Heirs no. 3 well	28
5	SEM image of a sample from a depth of 2,536.5 feet in the Campbell Heirs no. 3 well shows quartz overgrowths, pore throats, grain distribution, and precipitation of diagenetic iron-rich chlorite	29
6	SEM image of another area of the sample shown in plate 5 shows dissolution of plagioclase and possible precipitation of albite overgrowths	29

ABSTRACT

Xenia East Field in Clay County, Illinois, was discovered in 1951. About 1 million barrels of oil (bbl) have been produced from five pay zones, including the Cypress Sandstone (Mississippian), which supplied about half of the total. Production from this zone was discontinued in 1978.

The reservoirs are interpreted to be marine bar sandstones. The Cypress pool trapping mechanism is predominantly structural, although both a structural near-shore bar play and a stratigraphic offshore bar play were identified in this field. Nearshore sandstones, when combined with structural closure, form the most important reservoir interval and contain almost all the reserves in the Cypress reservoirs.

Stacked marine bars form vertically and horizontally heterogeneous reservoirs. Porosities of the reservoirs are relatively consistent in the study area, whereas permeabilities vary from sample to sample. Thin section petrography and scanning electron microscopy/energy dispersive x-ray (SEM/EDX) analyses indicate that the major porosity is intergranular. Pores created by feldspar dissolution have enhanced permeability. Silica in the form of quartz overgrowths is the most common type of cement. Clay minerals, as determined by x-ray diffraction (XRD) analysis, consist of kaolinite, chlorite, illite, and mixed-layered illite/smectite. Clay content reduces reservoir permeability.

The initial oil saturation, as interpreted from electric logs (E-logs), ranges from 40% to 72%. Stock tank original oil in place (STOOIP) is estimated to be 2.02 to 2.54 million bbl by volumetric methods. There is a high potential for additional oil recovery from the Cypress pool because more than 75% of STOOIP remains and the reservoir has not been waterflooded. Between 360,000 and 570,000 bbl of remaining mobile oil may be producible, given a well designed secondary recovery program. Implementation should include infill drilling, perforating Cypress intervals in nonplugged existing wells, waterflooding, and proper completion and treatment procedures.

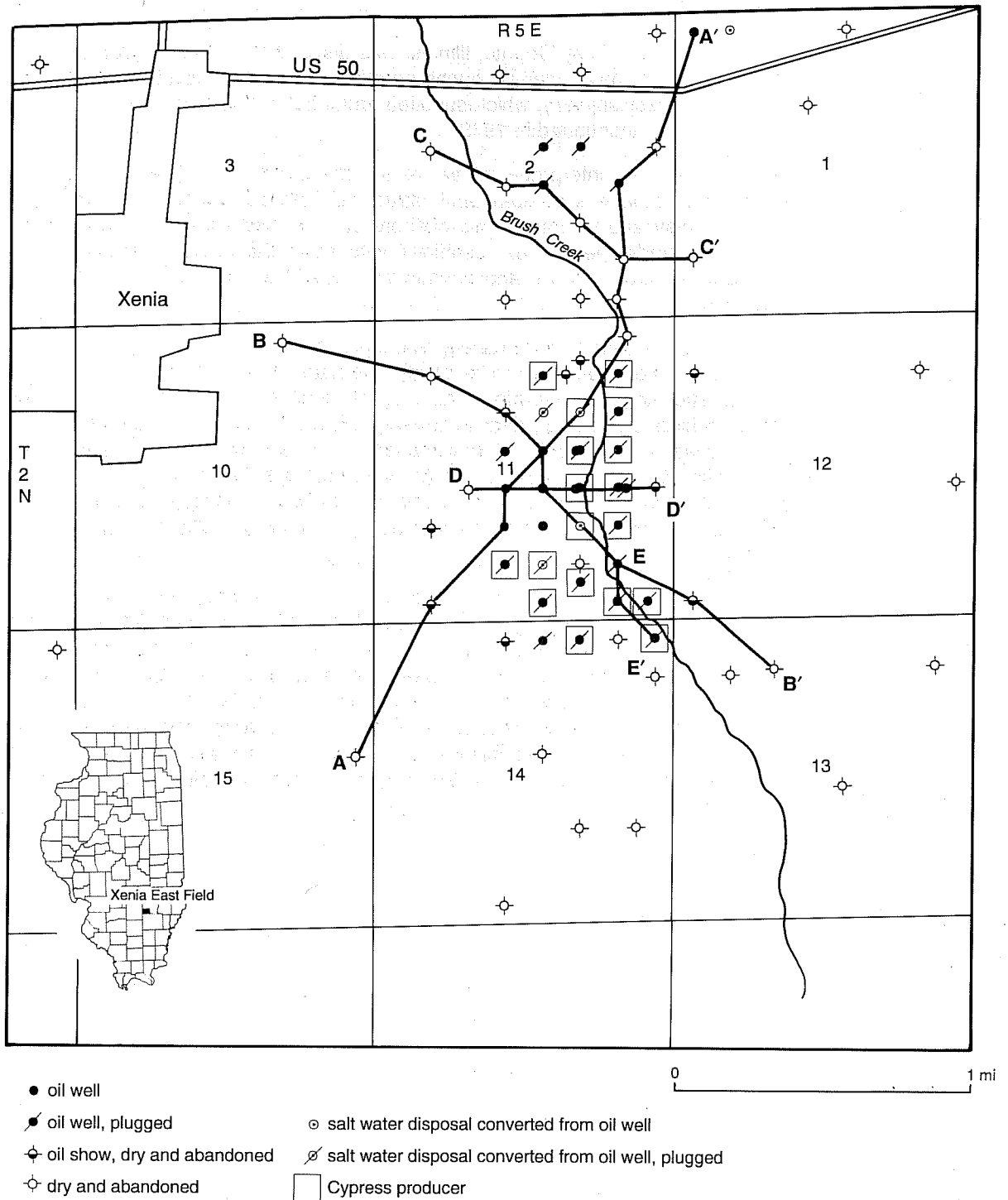


Figure 1 Locations and status of wells in Xenia East Field. Cross section lines A-A', B-B', C-C', D-D', and E-E' are also shown.

INTRODUCTION

Scope

The Xenia East oil field occupies about 1 square mile in southwest Clay County (Secs. 11 and 14, T2N, R5E), about 1.5 miles southeast of the town of Xenia (fig. 1). The study area is on a southeastward-dipping monoclinal slope that has only small structural relief between the Louden-Salem anticlinal trend and the Clay City Anticlinal Belt (fig. 2).

The goals of this study were to investigate the reservoir characteristics of the Cypress Sandstone at Xenia East Field, calculate the amount of original oil in place, and estimate the remaining mobile oil. This report also suggests techniques for recovering additional oil from the field.

Data used in this study include electric logs (E-logs, including resistivity and spontaneous potential logs) and drillers' reports from 70 wells in the field area. Core analysis, thin section petrography, scanning electron microscopy/energy dispersive x-ray (SEM/EDX) analysis, and x-ray diffraction (XRD) analysis techniques were used on some well cuttings from Cypress Sandstone, as well as on some plugs from one set of 23 core plugs.

Discovery and Development History

Xenia East Field was discovered in 1951 with the completion of the G.G. Campbell no. 1 well (SE NW SE, Sec. 11, T2N, R5E). This well initially produced 45 barrels of oil per day (BOPD) and 24 barrels of water per day (BWPD) from the Mississippian Cypress Sandstone at a depth of about 2,550 feet. During subsequent field development, the Mississippian Bethel, Renault, and Aux Vases Formations, and the "McClosky limestone" of the Ste. Genevieve Formation were also found to be oil-bearing (fig. 3). By 1963, 18 Cypress wells had been completed on a 10-acre well spacing; 15 wells produced open hole and seven were fractured (table 1). Three of the four salt-water disposal wells in the field were converted from Cypress production wells. Only two of these actually injected salt water into the Cypress Formation; the third injected water into the Tar Springs Sandstone. In addition to the 18 Cypress producers, 12 wells in the field produced from other formations.

Cypress wells at Xenia East initially produced oil at a high rate, and more than half of the total produced oil was extracted within 3 years of discovery. Early Cypress production peaked at 100,000 barrels of oil (bbl) in 1952, then began to decline (fig. 4). Three Cypress wells were drilled in 1963 and increased the 1964 Cypress production to 10,000 bbl per year. Two of these wells were drilled to develop the southeastern part of the field. A third well, the East Central Developing Company, Inc., Goad no. 1 (SW SE SE, Sec. 11, T2N, R5E), was completed in an additional Cypress pay zone. When production from the Cypress ceased at Xenia East Field in 1978, cumulative production had reached 470,000 bbl (Gerrish 1988).

Production from all producing formations in the field reached about 999,000 bbl by April 1991. The 30 producing wells have each averaged more than 33,000 bbl. Current production from the entire field is 5 BOPD (Petroleum Information 1991). None of this is from the Cypress.

RESERVOIR AND TRAP CHARACTERISTICS

Stratigraphy

In this area, the Chesterian Series consists of interbedded limestone and shale units that alternate with interbedded sandstone and shale units from the top of the Renault Formation (fig. 3) up to the major unconformity at the base of the Pennsylvanian

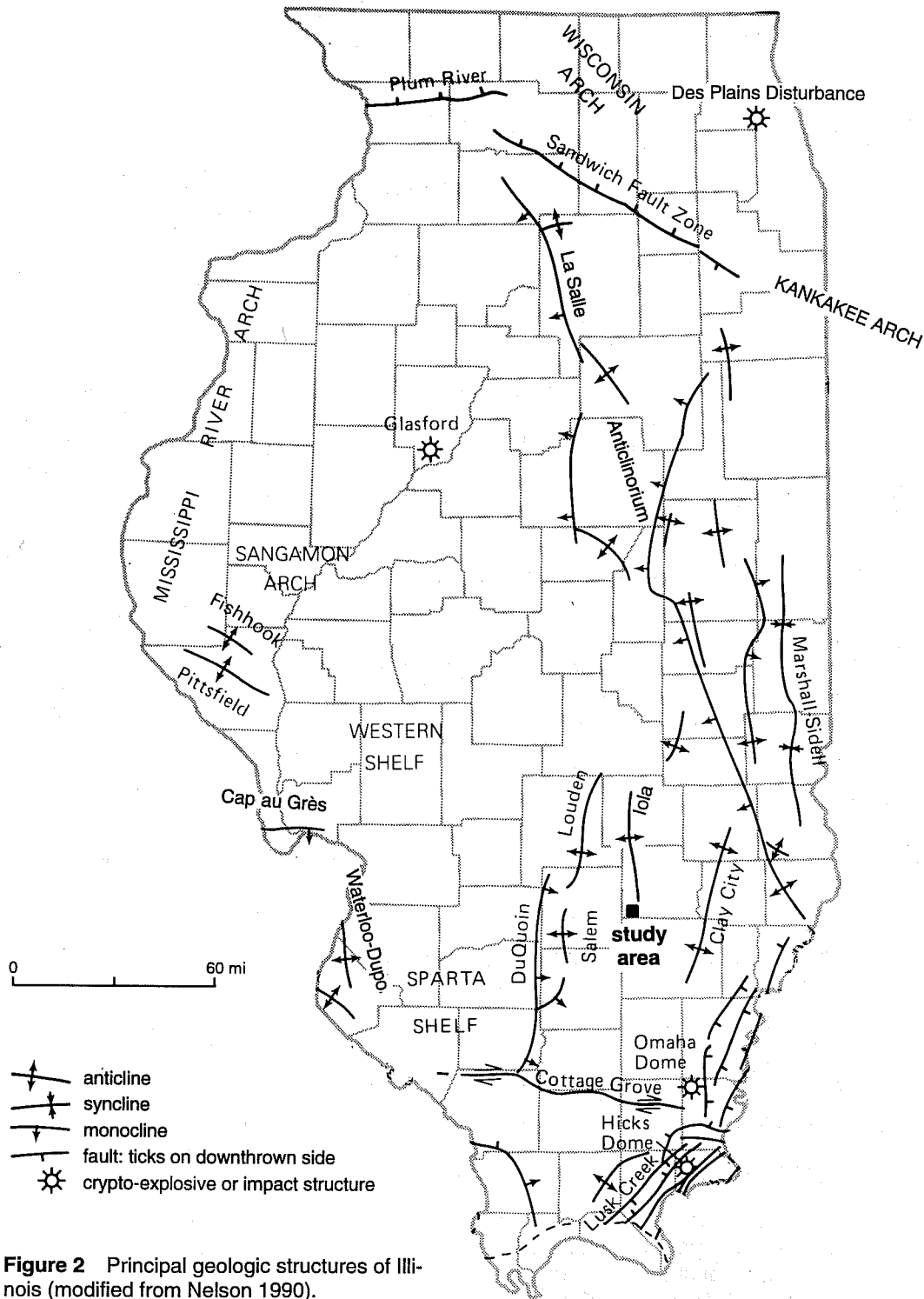


Figure 2 Principal geologic structures of Illinois (modified from Nelson 1990).

System. The Cypress Sandstone, one of the thickest and most persistent sandstone formations of the Chesterian (Willman et al. 1975), is overlain by the Beech Creek Limestone (informally the "Barlow limestone") and underlain by the Ridenhower Formation. The contact between the Cypress and the Ridenhower is generally conformable, but the Ridenhower is truncated locally where Cypress deposition scoured channels.

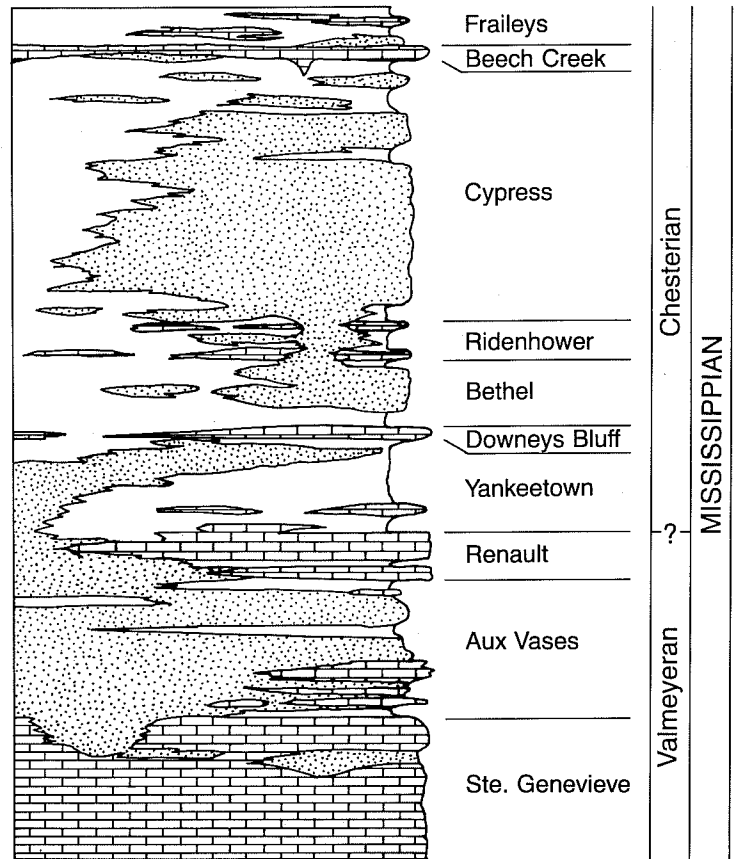


Figure 3 Generalized stratigraphic column of southern Illinois Basin (after Whitaker and Finley 1992).

Table 1 Production and completion information for Cypress wells in the study area

Well name	County number	Location			Date completed	Date plugged	Completion type	Treatment	Initial production		Date converted to SWD	
		Sec.	1/4	1/4					1/4	BOPD		BWPD
Baity, H. no. 1	1213	11	SW	NE	SE	6-52	1-56	open		32	7	
Bennett no. 1	2033	11	E ¹ / ₂	SW	SE	5-52	1-56	open	fracture	70	14	
Bible-Stoops Comm. no. 1	2034	11	NW	SW	SE	8-51	5-65	open		47	40	8-55
Bible-Stoops Comm. no. 2	2035	11	SW	SW	SE	10-51	7-64	open		47	24	
Bryan, Schel no. 1	2048	14	NE	NW	NE	10-51	4-65	open		36	60	
Campbell, G. no. 1	2036	11	SE	NW	SE	7-51		open		45	24	5-63
Campbell, G. no. 2	2037	11	NE	NW	SE	6-52		open	fracture	56	10	
Flick, W.C. no. 1	2038	11	NE	SE	SW	7-52	10-57	perforate	fracture	42	85	
Goad no. 1	1992	11	SW	SE	SE	11-63	9-78	open	fracture	47	0	
Goad no. 2	2017	11	SE	SE	SE	12-63	10-64	open	fracture	25	100	
Goad Comm. no. 1	1974	14	NE	NE	NE	8-63	10-64	open	shot	25	50	
Goad, E.M. no. 1	2040	11	SE	SW	NE	10-51		open		49	6	
Goad, E.M. no. 2	2041	11	NE	SW	NE	11-51		perforate		75	6	7-65
Shoots-Woomer no. 1	1454	11	SW	NW	NE	2-60	7-60	perforate		8	5	
Woomer, I., no. 2	2046	11	SW	SE	NE	8-51	2-82	open		70	0	
Woomer, I. no. 3	2047	11	NW	SE	NE	7-52	7-58	open		152	6	
Woomer, E.J. no. 2	2044	11	SW	NE	NE	6-52	1-56	open	fracture	96	0	
Woomer, E.J. no. 3	2045	11	NW	NE	SE	9-52	1-56	open	fracture	80	0	

The Cypress Sandstone reaches a maximum thickness of 160 feet in the study area (fig. 5); 50% to 70% of the total Cypress interval is clean sandstone, locally as much as 130 feet thick (fig. 6). A "clean" sandstone is defined as having an SP response that is at least 50% of the SP response of the Chesterian Tar Springs Sandstone, which is the standard clean sandstone in this area. A "dirty" sandstone has an SP response between 25% and 50%.

Seven sand bodies were identified, on the basis of well log correlations, in the Cypress Sandstone at Xenia East Field. From the top down, the units were numbered 1 to 7 (figs. 7–10). The upper part of the Cypress (units 1–6) is more shaley than the lower part (unit 7) and consists of thin sandstone units interbedded with shale. Unit 7, which consists of thick sandstone with thin shale breaks, makes up about half of the total thickness of the formation (figs. 7–10). Unit 4 is the major pay zone for the Cypress Sandstone at Xenia East Field, but there is also minor oil production from unit 2. Shows of oil have been reported in units 5 and 6.

Reservoir Geometry

The Xenia East Field lies on the Kenner Anticline, which is roughly aligned with the Iola Anticline (figs. 2, 11). The structure appears consistently in major mapping horizons, but the crests on other horizons are not coincident with the structure in the Cypress Sandstone. The thickest sandstone in the Cypress lies on the crest of the Kenner Anticline. Consequently, both structural activity and differential compaction of sandstones and shales probably contributed to the morphology of the anticline.

The term reservoir, as used in this report, refers to a zone or horizon that has the lithologic characteristics of an oil-producing zone. Although units 2 and 4 are the only Cypress pays in the field, all the Cypress Sandstone units, except unit 1, are considered to be part of the reservoir.

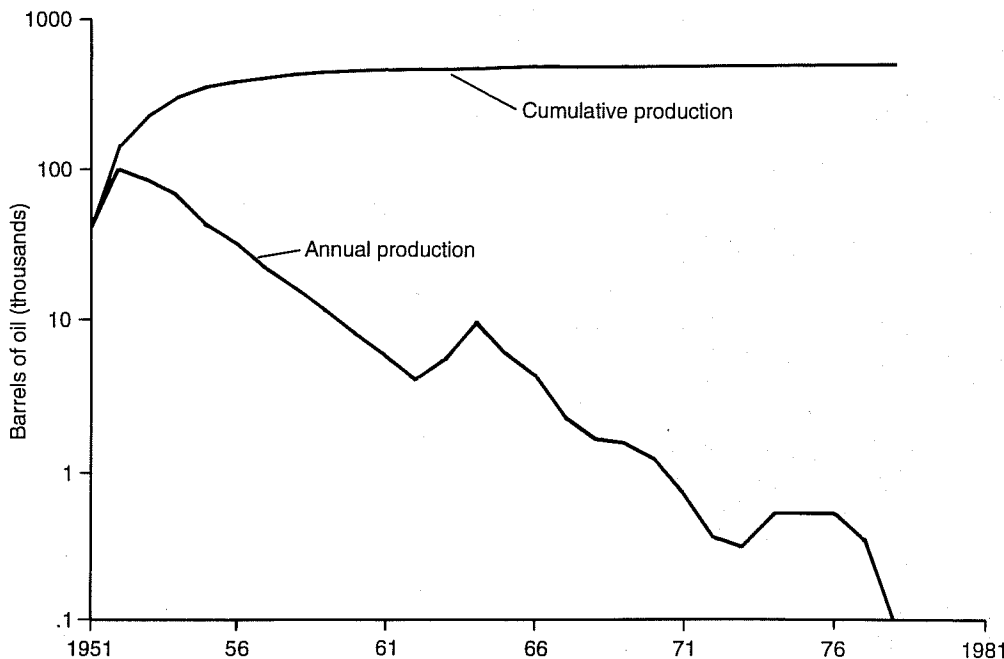


Figure 4 Production curves showing the decline that began the second year after the discovery of Xenia East Field (after Gerrish 1988).

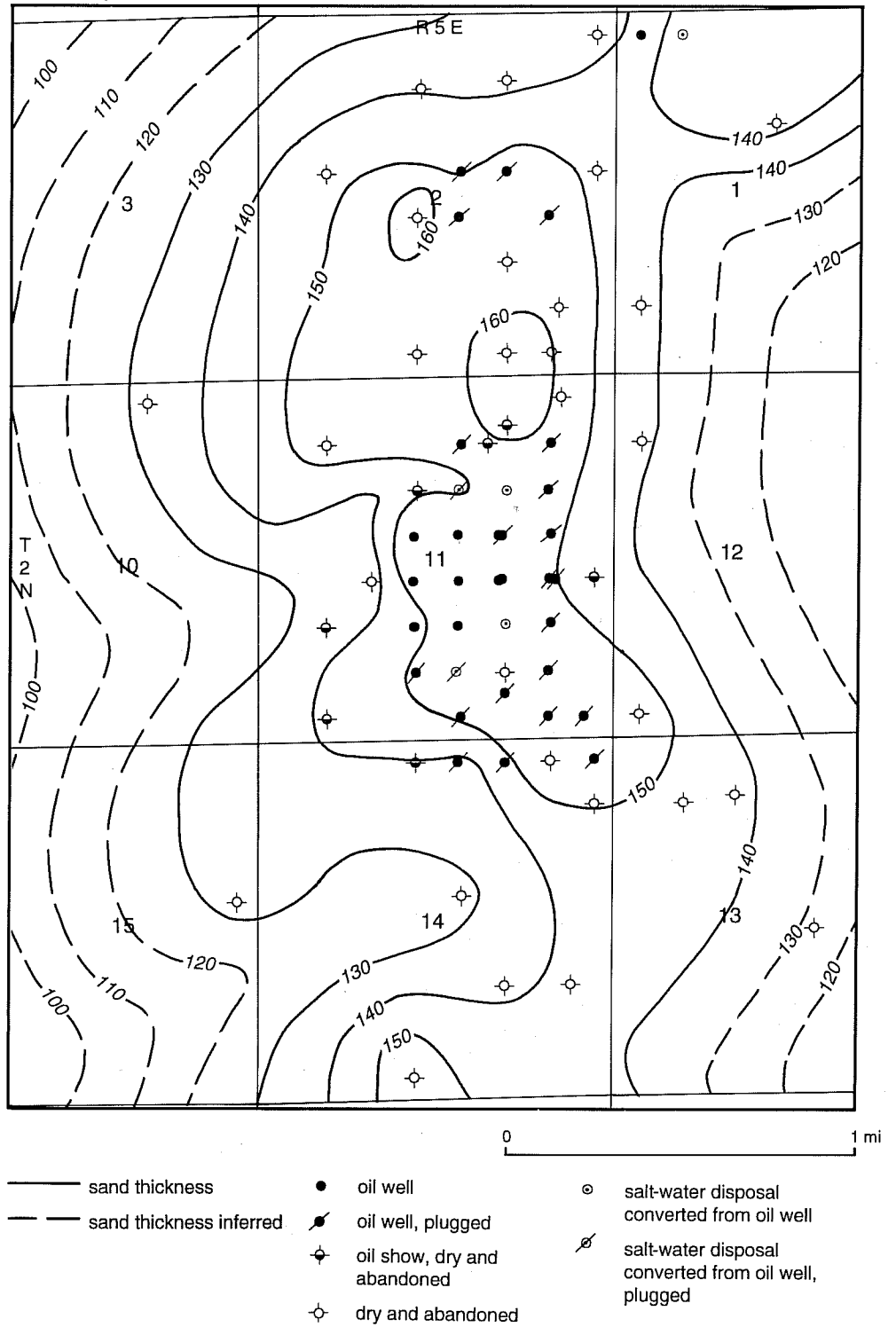


Figure 5 Thickness map of Cypress Sandstone at Xenia East Field. Contour interval is 10 feet.

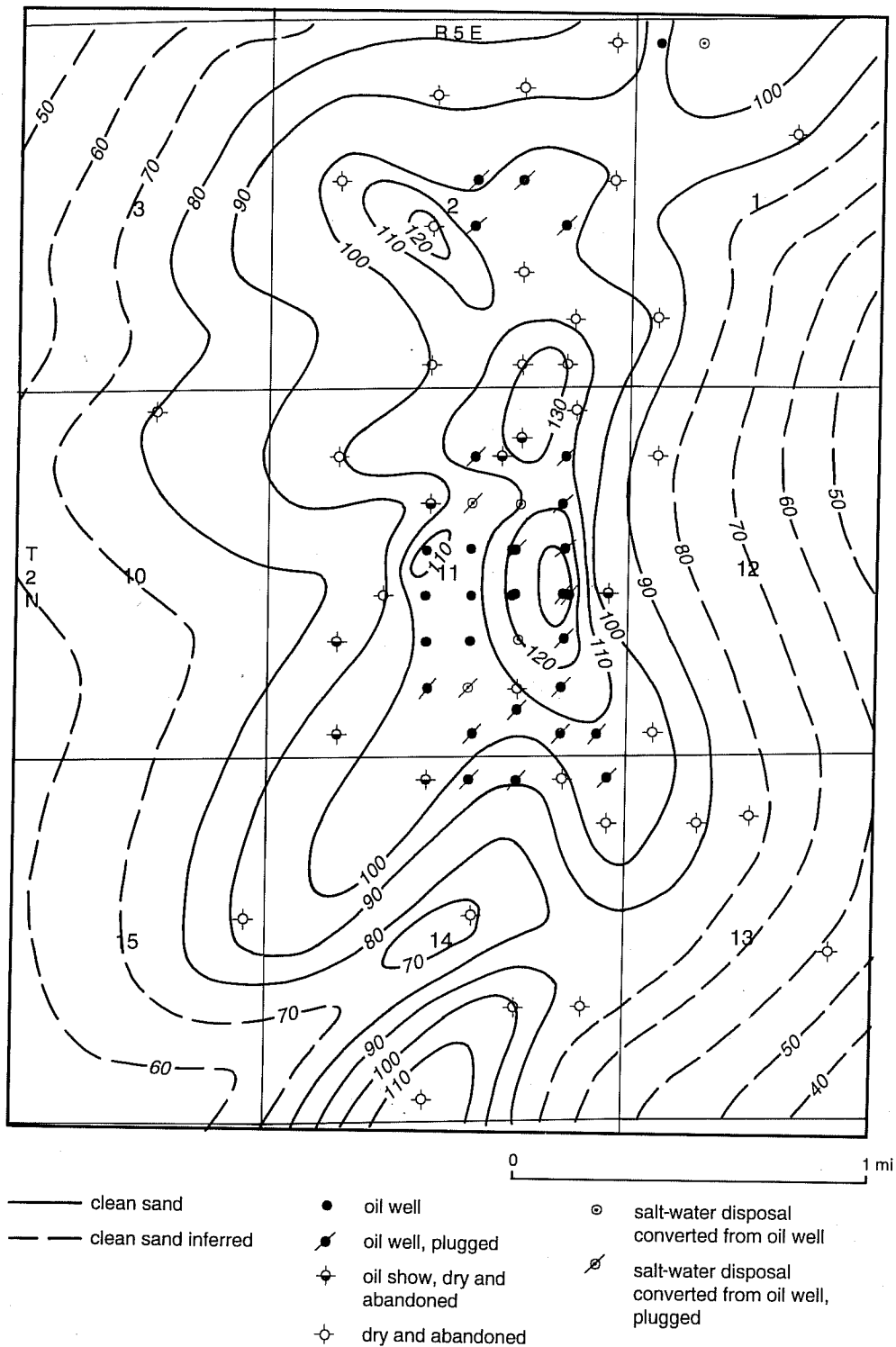


Figure 6 Total thickness of clean sandstone in the Cypress Sandstone at Xenia East Field. The thickest sand lies along the structural crest. Contour interval is 10 feet.

National Assoc.
Bryan, Schel no. 1
2048

Ward W. Dayton
Goad, E.M. no. 2
2041

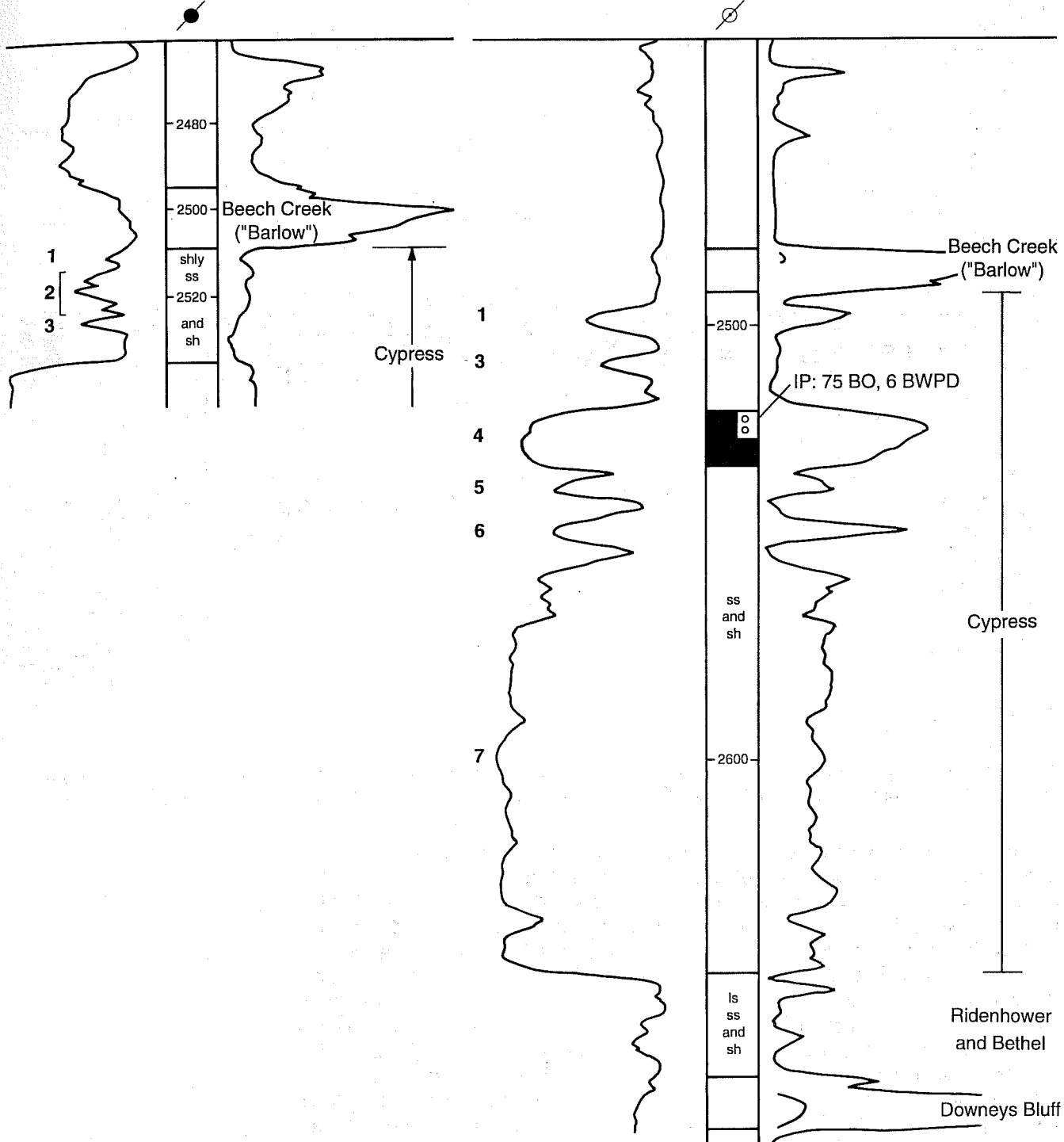


Figure 7 Typical E-logs showing the subdivision of sandstone units 1 to 7 of the Cypress Formation at Xenia East Field.

S

A

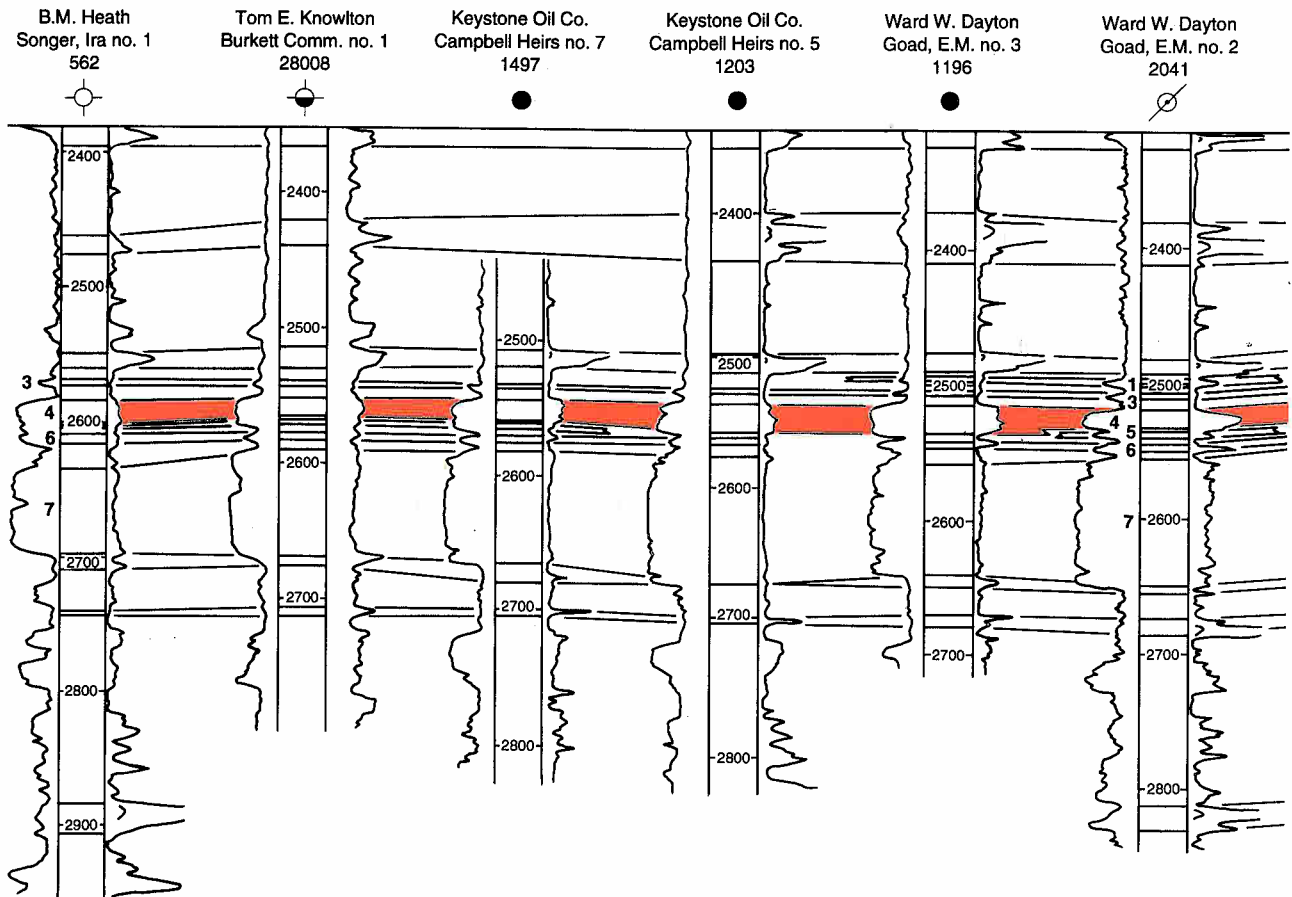
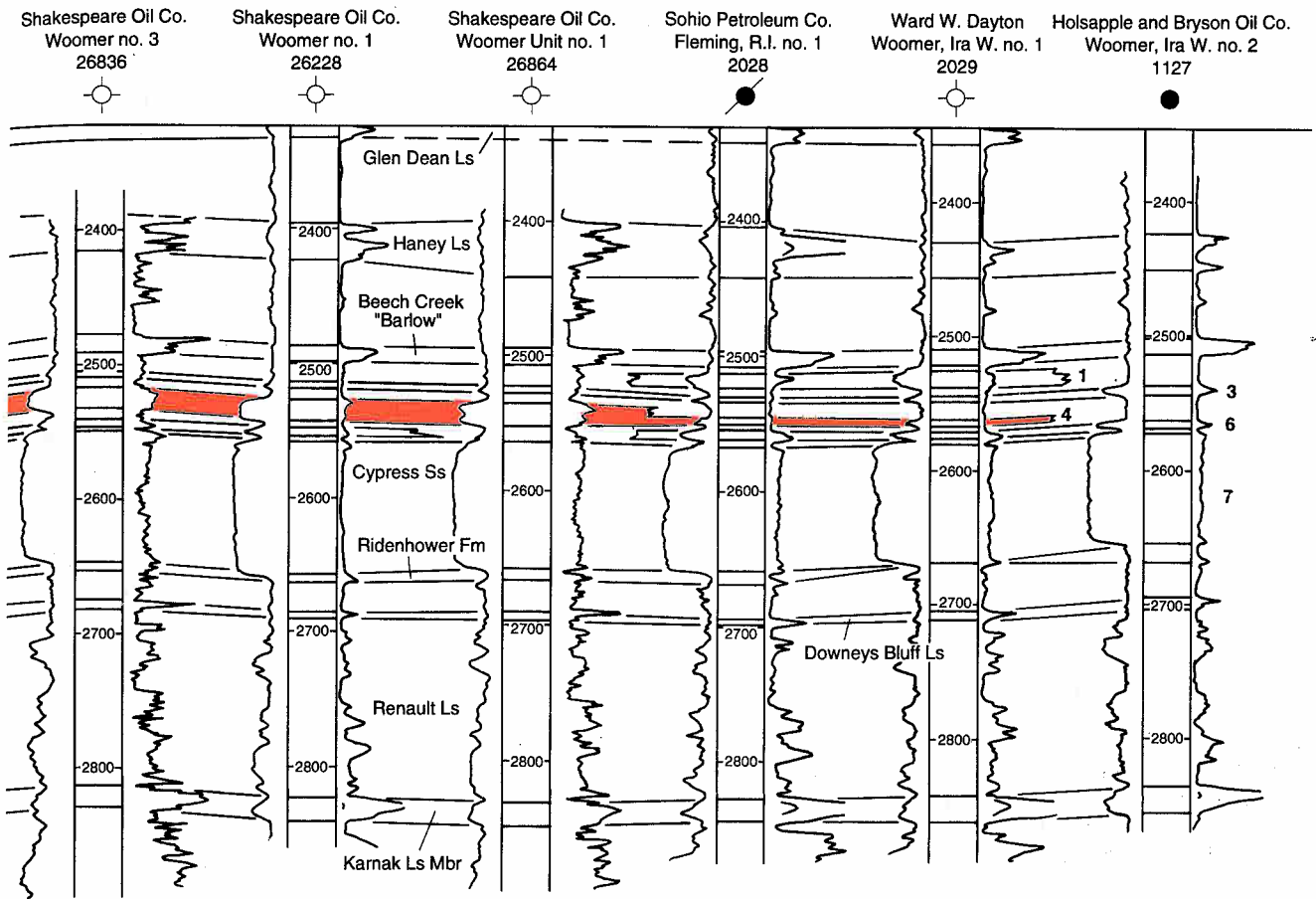


Figure 8 Stratigraphic cross section A-A' (see fig. 1) showing the connection and distribution of sandstone units along a north-south line. Datum is the top of the Glen Dean Limestone. Unit 4, the oil-producing zone, is highlighted in red.

The elongation of the sand bodies occurs in two directions: north to south in units 6 and 7 and north-northeast to south-southwest in all other units. Unit 7, a highly complex sand body present throughout the mapped area (figs. 8-10), is about 3 miles long and 2.5 miles wide; it increases in both thickness and width to the north and south of Xenia East Field in Section 11 (fig. 12). Unit 6 occupies a smaller area (3 miles long and about 1.5 miles wide) than does unit 7. Most of it lies along a north to south elongation axis (fig. 13). Unlike the nearly constant thickness of unit 7 (shown in the cross sections), unit 6 is wedge-shaped and pinches out eastward (figs. 9, 10). Units 1 to 5 are narrow (more than 1 mile long and 0.3-1.5 miles wide) and lenticular in cross section. Their elongation axes trend north-northeast, and their greatest thicknesses are largely coincident with the structural crest in Xenia East Field (figs. 11, 14-18). Units 2 to 5 each consist of two parallel sand bodies, as illustrated by unit 5 (fig. 14), but the thickest parts of the units do not exactly coincide.

Trap Type

Two types of traps were identified in the Cypress at Xenia East Field, one structural (fig. 19) and the other stratigraphic (fig. 21). Oil is structurally trapped in unit 4, which contains almost all the Cypress oil reserves in this field (figs. 15, 19). The isopach map of the unit 4 pay zone (fig. 20) shows that commercial production was established only where the pay zone is thicker than 5 feet. The structure map on



the top of the Barlow limestone indicates that structural closure is about 19 feet. The crest of the structure on the top of the reservoir sandstone is slightly offset from the crest of the Barlow limestone structure because of the different sandstone thicknesses. Consequently, the reservoir sandstone in the East Central Developing Company, Baltrukonis no. 1 well (SW SW SW, Sec. 12, T2N, R5E) is below the oil-water contact, although it is located on the structural high of the Barlow limestone (fig. 20).

A stratigraphic trap controlled by the distribution and thickness of clean sand in unit 2 was found when the East Central Development Company's Goad no. 1 well (SW SE SE, Sec. 11, T2N, R5E; figs. 17, 21) was drilled. This is the only example of this trapping mechanism. Adjacent wells do not contain clean unit 2 sand and are not productive from this unit; however, this well contributed about 19,000 bbl to the field's cumulative production of 470,000 bbl from the Cypress.

Reservoir Lithofacies

Reservoir lithofacies descriptions and analyses of reservoir characteristics were partly determined from studies of drill cuttings from nine wells. Because pay zone cuttings were unavailable for the open-hole Cypress producers, most of the drill cuttings used in the study came from non-Cypress producers. One core from the

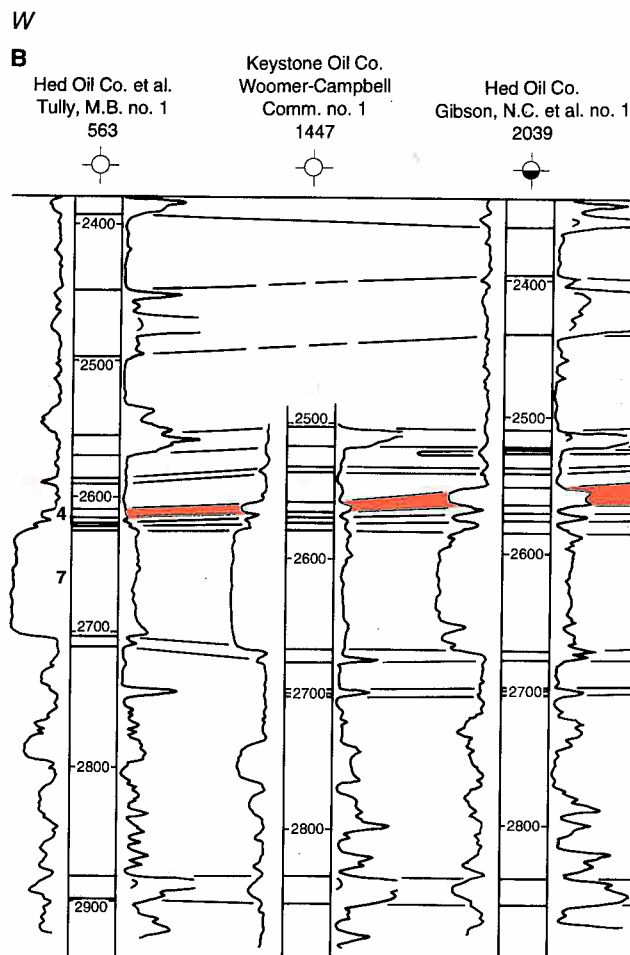
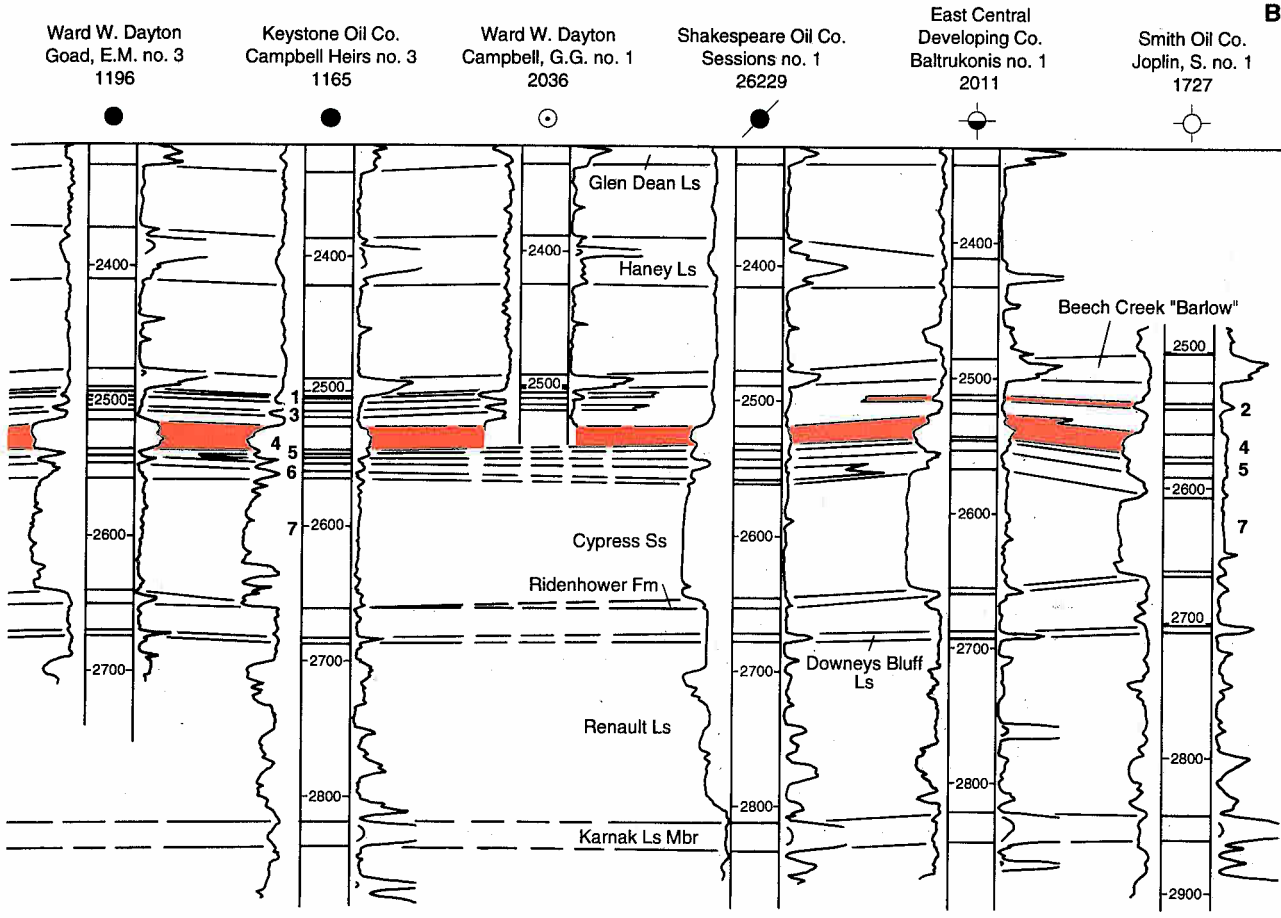


Figure 9 Stratigraphic cross section B-B' see (fig. 1) showing the connection and distribution of sandstone units along an east-west line in the center of the field. Datum is the top of the Glen Dean Limestone. The oil-producing zones, units 2 and 4, are highlighted in red.

upper Cypress in the Keystone Oil Company's Campbell Heirs no. 3 well in the central part of the field (NW NW SE, Sec. 11, T2N, R5E) provided 23 small-diameter plugs; eight were prepared as thin sections and analyzed by XRD. Three were examined using SEM/EDX. Conventional porosity and permeability analyses were performed on all 23 plugs. Thin sections also were made from the drill cuttings.

Both the upper and lower sandstone units are composed of quartz arenite. The sandstones in units 6 and 7 are a white, fine grained quartz arenite that is clean and friable. Framework grains are well to moderately sorted and subangular to subrounded. At the bottom of unit 7, the sandstone is greenish and contains more clay; carbonaceous shale and plant fossils are also common.

Units 4 and 5 are composed of light greenish to light gray, fine to very fine grained, clean quartz arenites that have low-angle crossbedding (plates 1 and 2). Clay laminae occur along bedding planes, and patchy occurrences of clay are common in some core plugs. Shales interbedded with these sandstone units, as represented in cuttings from throughout the study area, are red, indicating a state of high oxidation. Shows of oil are common in cuttings from the field. In the thin sections and SEM photomicrographs, framework grains are subrounded, moderately to well sorted and have point to straight grain contacts. Zircon, anatase, and hornblende (plate 2) are the most common heavy minerals found in the samples. Quartz overgrowths are common and their euhedral crystal edges are responsible for the angular grain outlines shown in plates 3 to 5. Quartz grains in the sandstone are clean, and no clay coatings are present on the original grain boundaries. Some grains are coated with iron oxide (hematite) underneath quartz overgrowths (plate 3).



X-ray diffraction analyses of clean sandstone samples show that quartz constitutes 90% or more of the bulk mineral components, feldspar less than 8%, and clay less than 3%. Calcite and dolomite occur in trace amounts (table 2).

Units 1, 2, and 3 are composed of gray to greenish siltstone and very fine grained quartz arenite. Cuttings are dense, and their greenish color indicates the sands are rich in clay matrix. Net clean sands in these units are only present in some areas.

The 23 core plugs from Keystone's Campbell Heirs no. 3 well were taken in unit 4 and unit 5 sandstones at 1-foot intervals from 2,525.5 to 2,548.5 feet. Porosity values, ranging from 13.5% to 17% (average 15.3%) from sample to sample, do not differ significantly. Conversely, permeabilities show a large variation from 4.4 to 88 md (average 37 md); the modal value is about 60 md. Because the plot of permeability relative to depth generally mimics the shape of the SP-log (fig. 22), it seems likely that permeability is affected by the clay matrix content of the rock. The low permeabilities at the top and bottom of the reservoir are probably caused by compaction of oriented grains, finer grain size, and large amounts of calcite cement. These features are common in shale-sandstone sequences and have been observed in many cores and thin sections from Cypress reservoirs throughout the Illinois Basin (Cole, ISGS, personal communication 1992). Observations of thin sections indicate that porosity values are nearly constant at about 15%.

Porosity is predominantly intergranular, and pores average about 50 μ m in width. Several types of dissolution pores, as defined by Schmidt and McDonald (1979), were identified (e.g., oversized pores, granular molds, and elongate pores). Second-

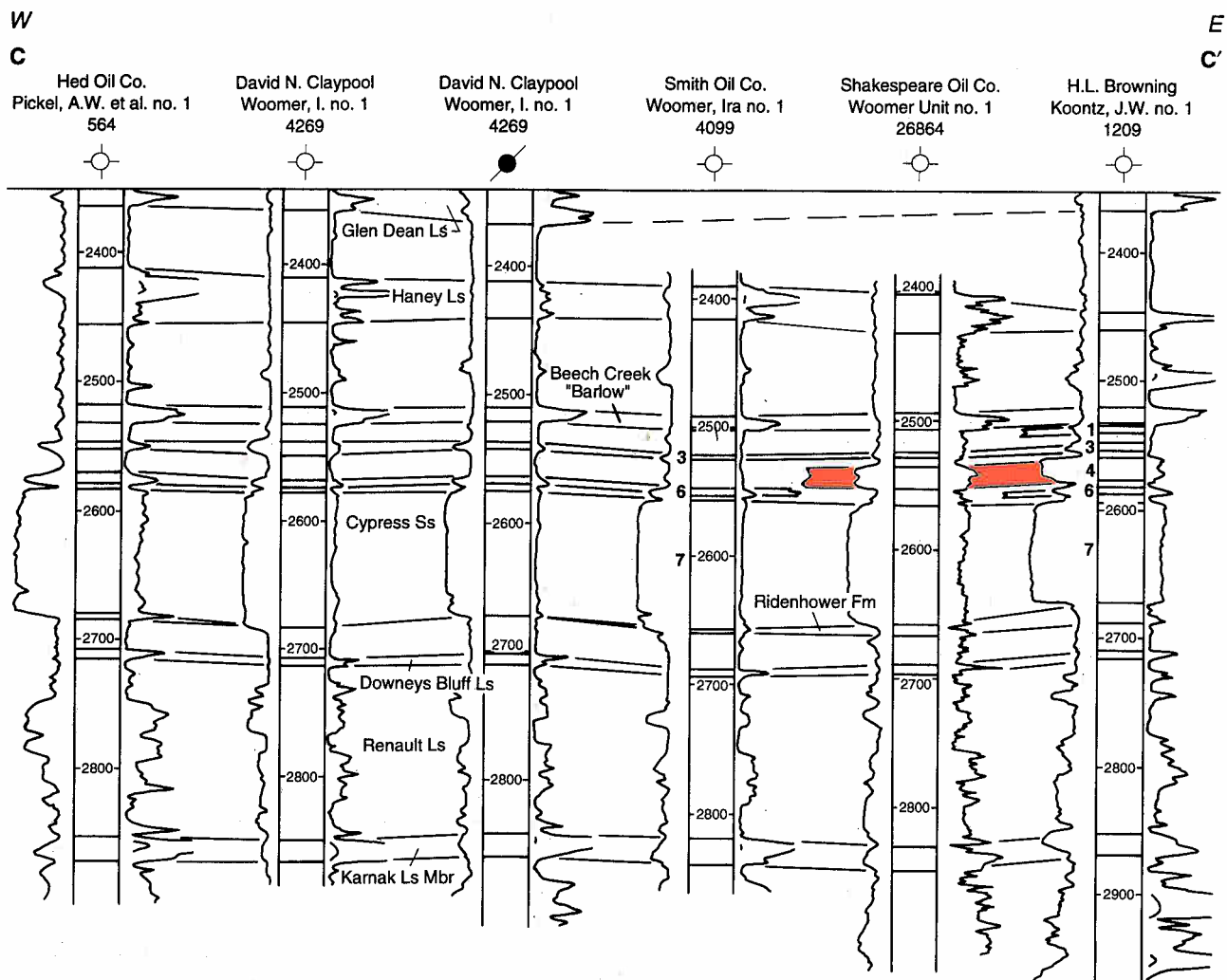


Figure 10 Stratigraphic cross section C–C' (see fig. 1) showing the connection and distribution of sandstone units along an east–west line in the north part of the field. Datum is the top of the Glen Dean Limestone. The oil-producing zone, unit 4, is highlighted in red.

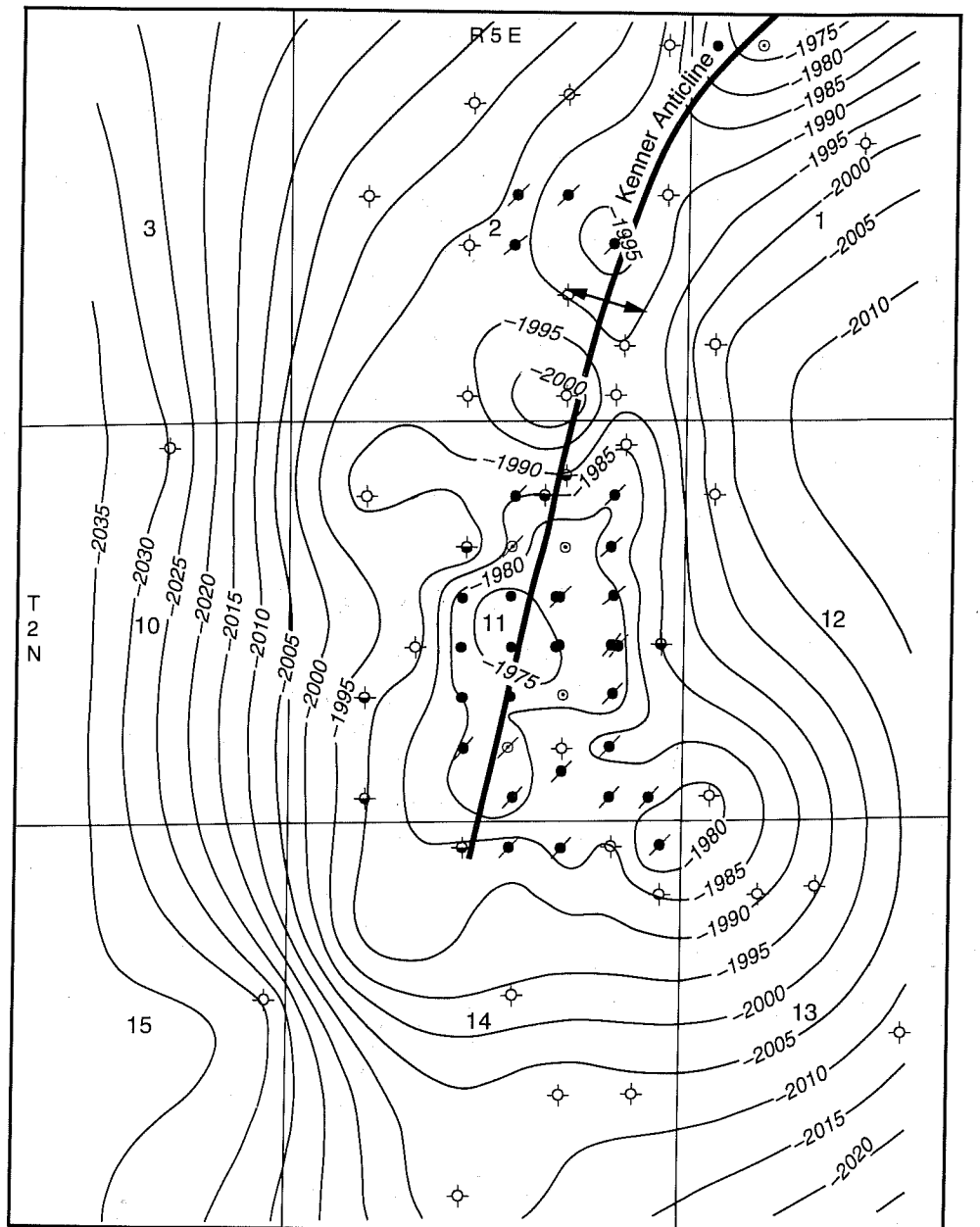
dary porosity has developed mainly from the dissolution of feldspar. Plates 4, 5, and 6 show examples of pores and feldspar dissolution in thin section and SEM views.

Clay minerals in the samples appear to be typical of Cypress reservoirs (Moore and Hughes 1991). Clay mineral varieties determined from the <16 μm separations of disaggregated sandstone include illite, mixed-layered illite/smectite, chlorite, and kaolinite. SEM/EDX analysis indicates that the chlorite is an iron-rich variety (fig. 23). Relative amounts of these clay minerals are shown in table 2; total clay content in the clean sandstone samples is less than 3% (fig. 24, table 2).

Three types of cement are present: silica, clay minerals, and calcite. Silica in the form of quartz overgrowths is the most common type (plate 3). Clay mineral cements are not evenly distributed. Calcite is sparsely distributed as patchy cement, which increases near the boundary of sandstone in the core.

Depositional Environment

The geometry of sandstone units, lithologic successions, and overall geologic setting indicate the sediments that became the Cypress Sandstone at Xenia East Field were delivered to and deposited in an extensive, shallow, marine environment



- oil well
- ⊘ oil well, plugged
- ⊕ oil well, dry and abandoned
- ⊖ dry and abandoned
- ⊙ salt-water disposal converted from oil well
- ⊗ salt-water disposal converted from oil well, plugged

Figure 11 Structure map contoured on top of the Beech Creek Limestone ("Barlow"). Contour interval is 5 feet.

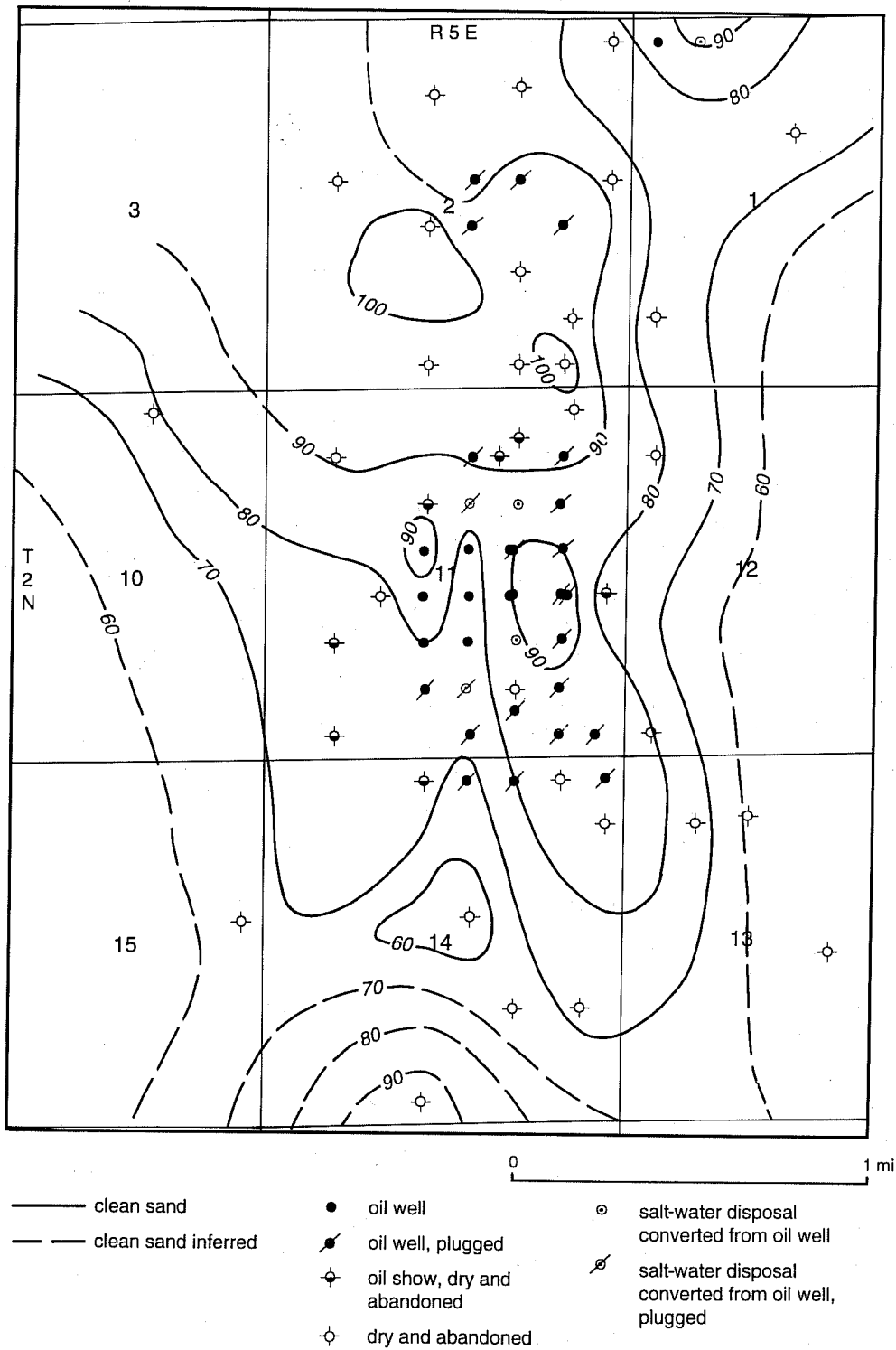


Figure 12 Thickness map of clean unit 7 sandstone. Contour interval is 10 feet. The axis of the sandstone body trends north to south.

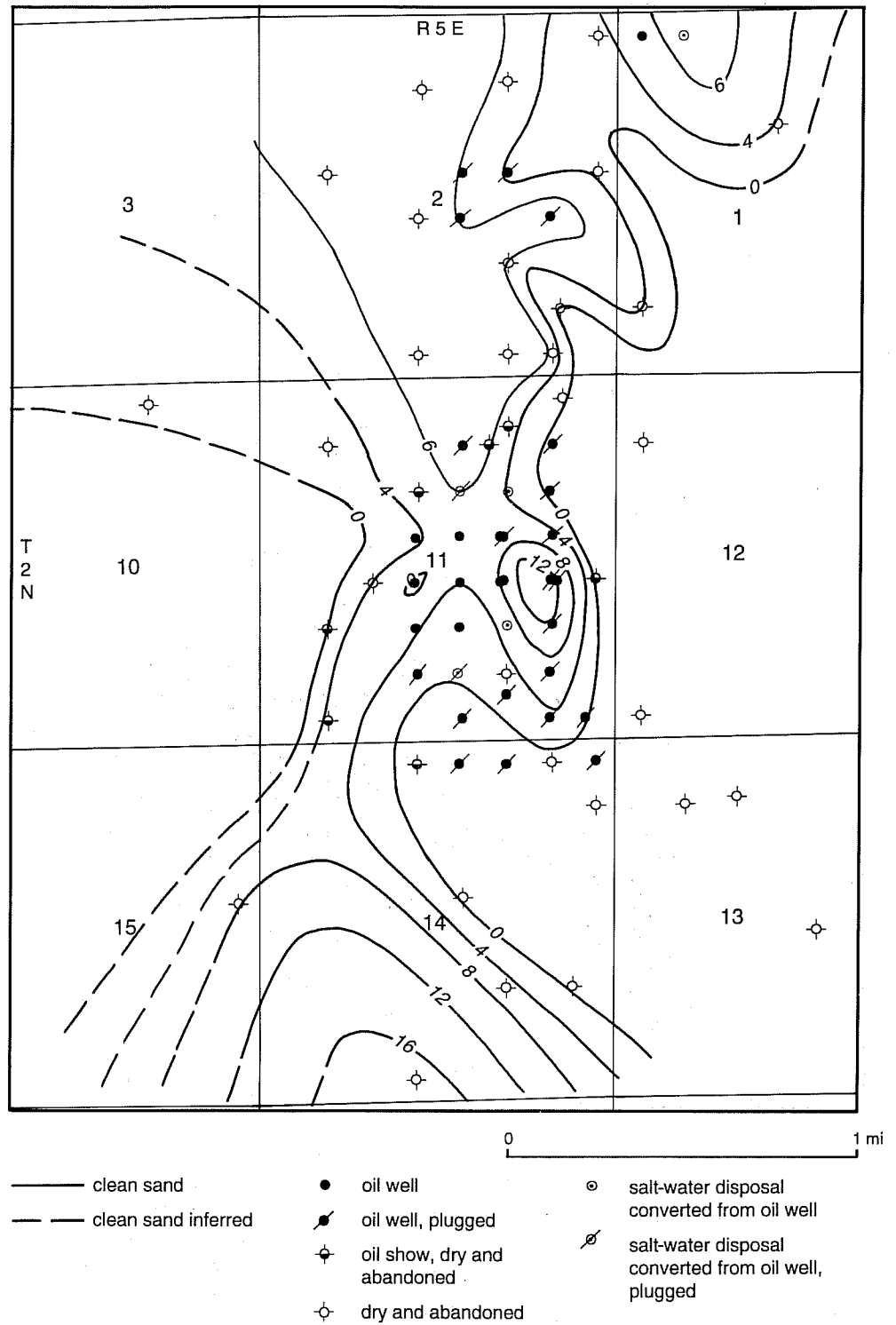


Figure 13 Thickness map of clean unit 6 sandstone. Contour interval is 4 feet.

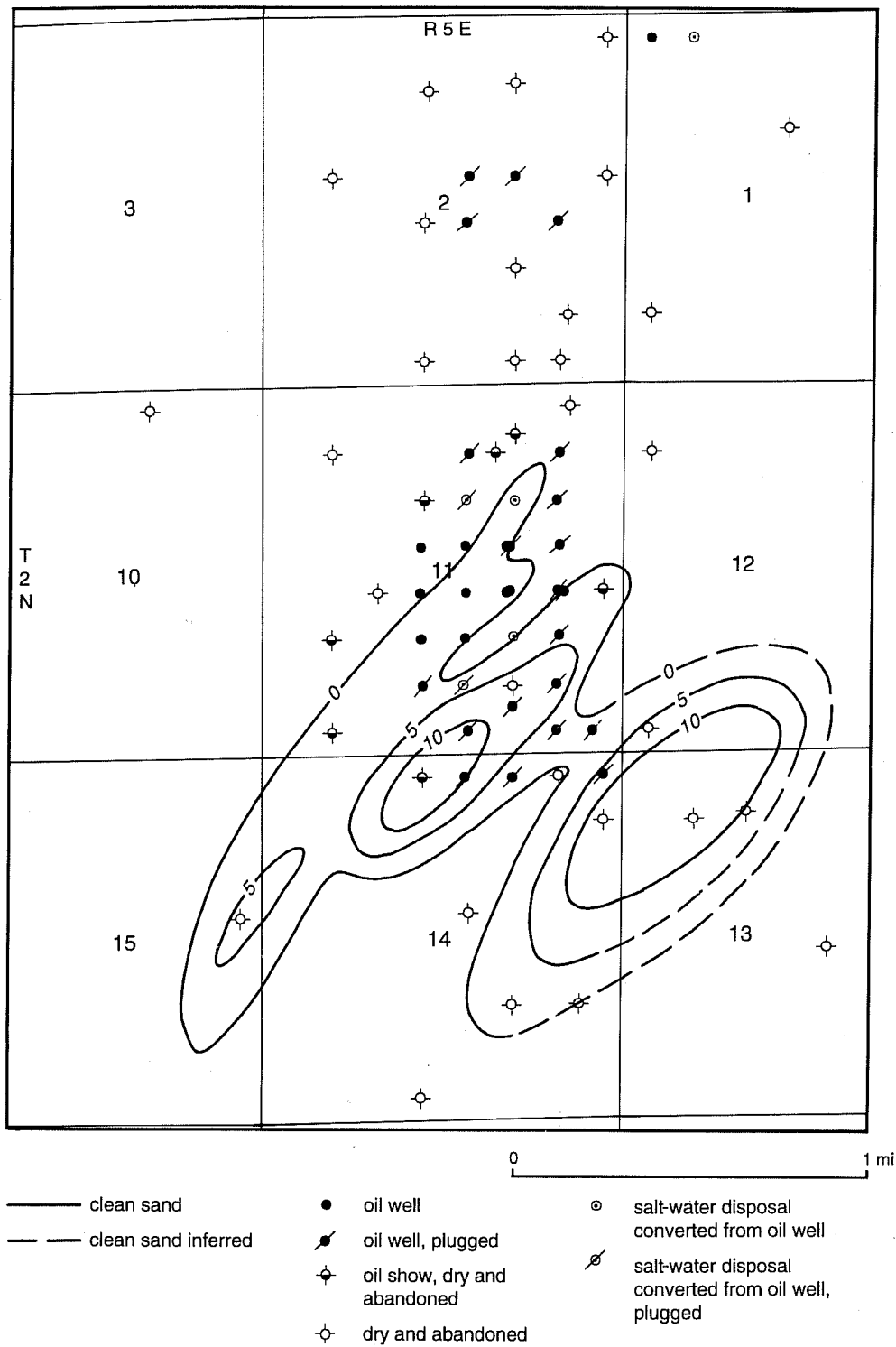


Figure 14 Thickness map of clean unit 5 sandstone. Contour interval is 5 feet. The orientation of the elongation axis of the sandstone bodies changes from north-south to northeast-southwest in this, and overlying Cypress Sand units.

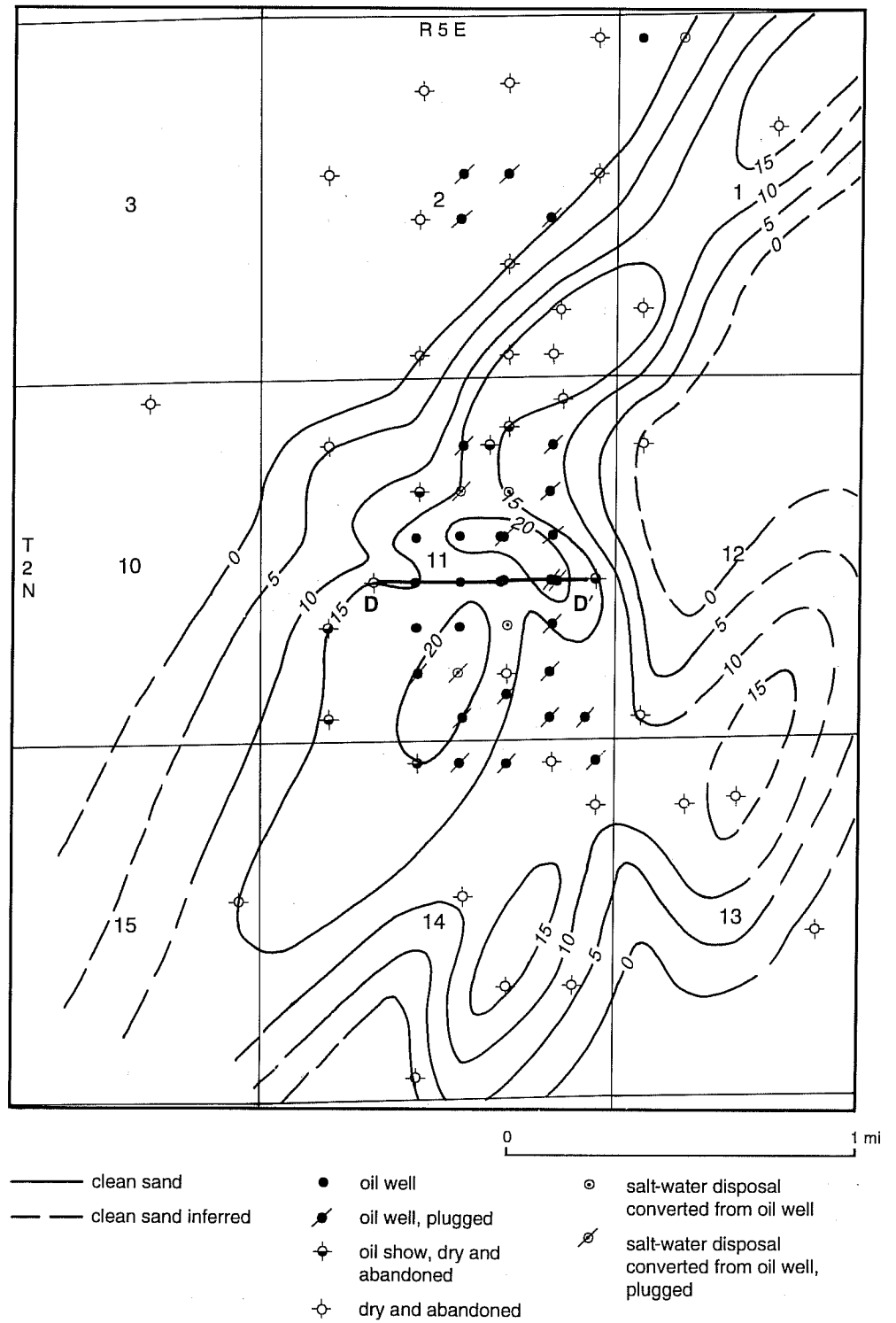


Figure 15 Thickness map of clean unit 4 sandstone. The line of cross section D-D' (see fig. 19) is also shown. Contour interval is 5 feet.

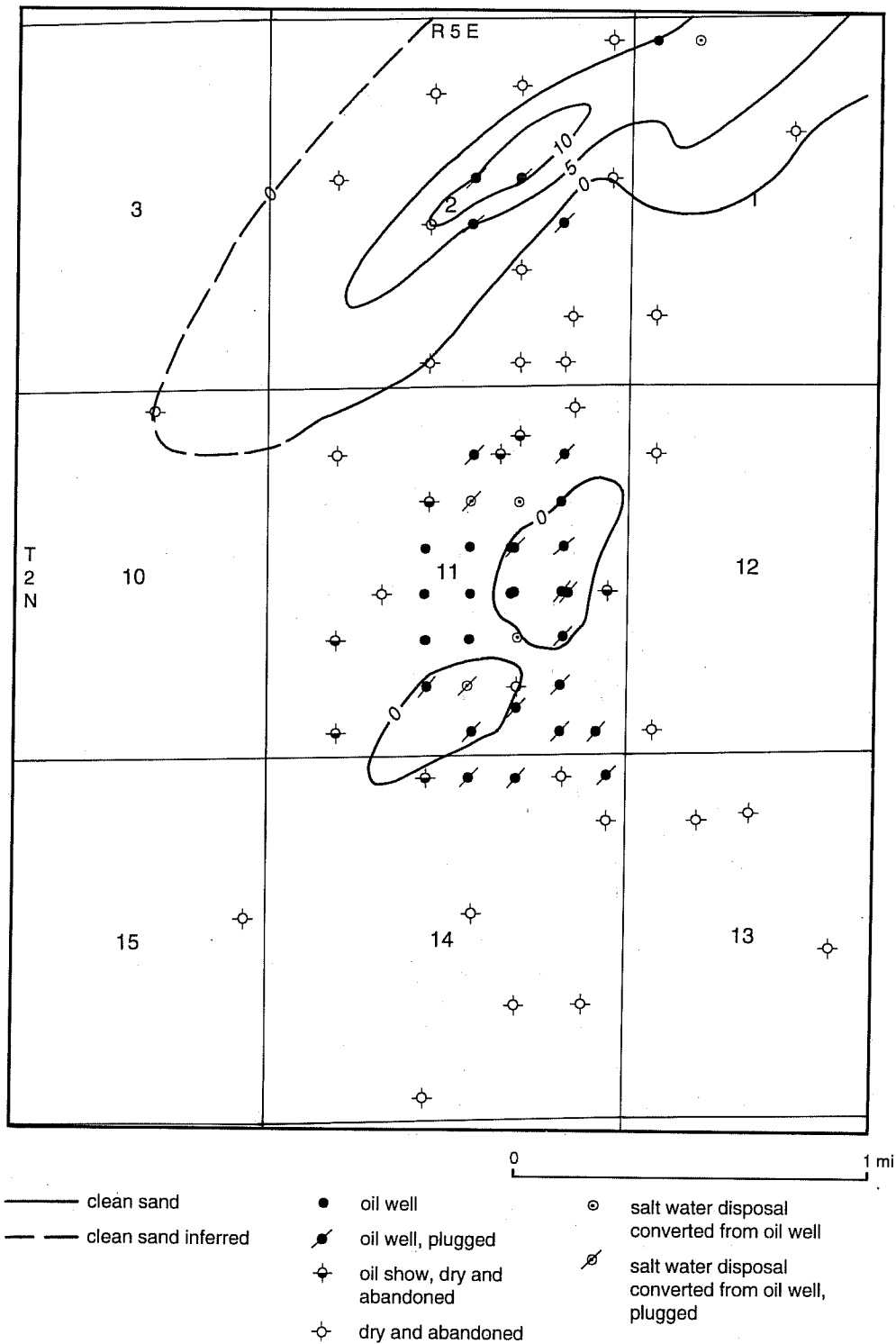


Figure 16 Thickness map of clean unit 3 sandstone. Contour interval is 5 feet.

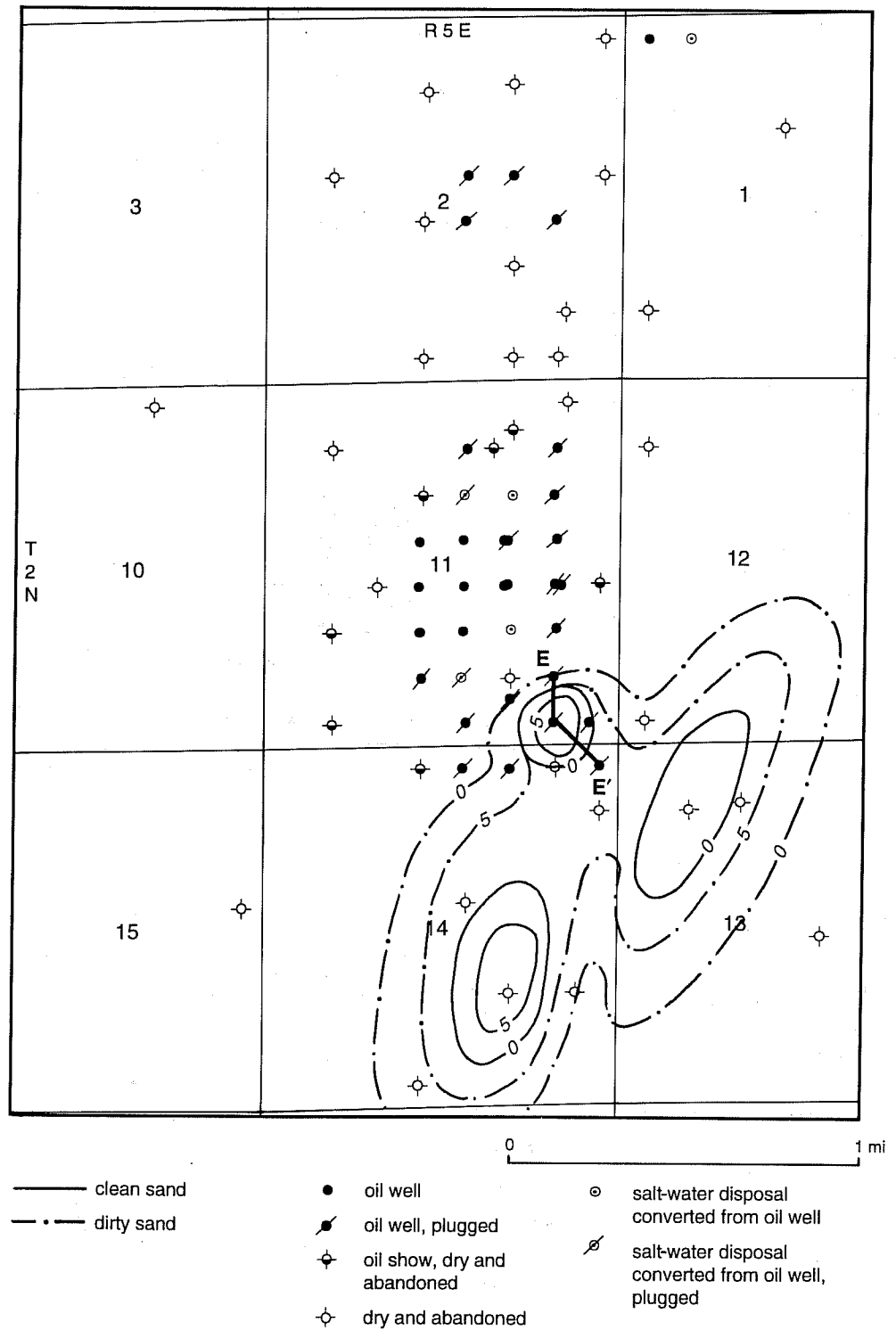


Figure 17 Thickness map of unit 2 sandstone. The line of cross section E-E' (fig. 21) is also shown. Contour interval is 5 feet.

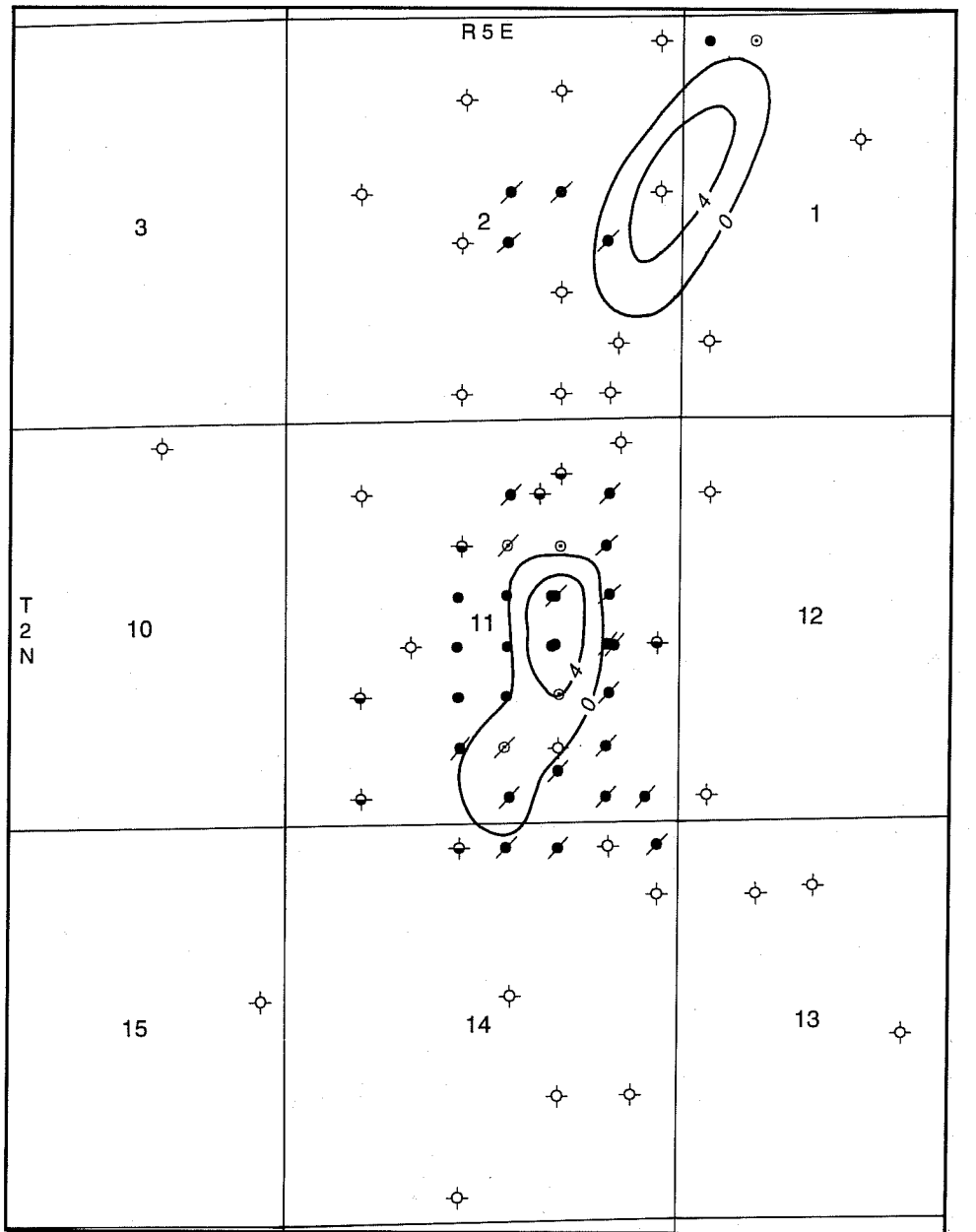


Figure 18 Thickness map of clean unit 1 sandstone. Contour interval is 4 feet.

in what is now the southern part of the Illinois Basin (Swann 1963). The characteristic features of units 6 and 7, including thickly bedded sandstone, carbonaceous shale, and plant fossils, are commonly associated with deposition near the mouth of a fluvial source. They could be interpreted as deltaic or estuarine sand bodies. Estuarine sandstones tend to be elongate in the flow direction, whereas the lobate form of the unit 6 and 7 sandstones is more characteristic of delta front sand bodies that were probably reworked by wave and tidal processes (Miall 1984). The thickness trends indicate that the source of clastic material was from the north (figs. 12, 13).

Unit 6 represents a transitional environment between units 5 and 7. It may have resulted from a shift in depositional geometry because the main body of unit 7 sandstone trends northward and the new sandbar (unit 5) formed with a north-northeast to south-southwest orientation.

The lack of fines and high degree of maturity of framework components in the unit 4 and 5 sandstones indicate that they formed in a relatively high energy environment. Their elongate, convex-upward lenticular shape (figs. 8, 9) and low-angle crossbedding are characteristic of marine bar sandstones (Davis 1978). The presence of red shale in this interval indicates a shallow water, oxidizing depositional environment. Because of these features, it is likely that the sandstones in units 4 and 5 were deposited as nearshore marine bars.

Units 1, 2, and 3 (siltstone and sandstone) are similar in geometry to units 4 and 5 but thinner and less extensive. Because these sand bodies lack clean sandstone and the sandstone to shale ratios are low in this interval, they are interpreted as having been deposited in a relatively low energy environment, possibly as offshore bars.

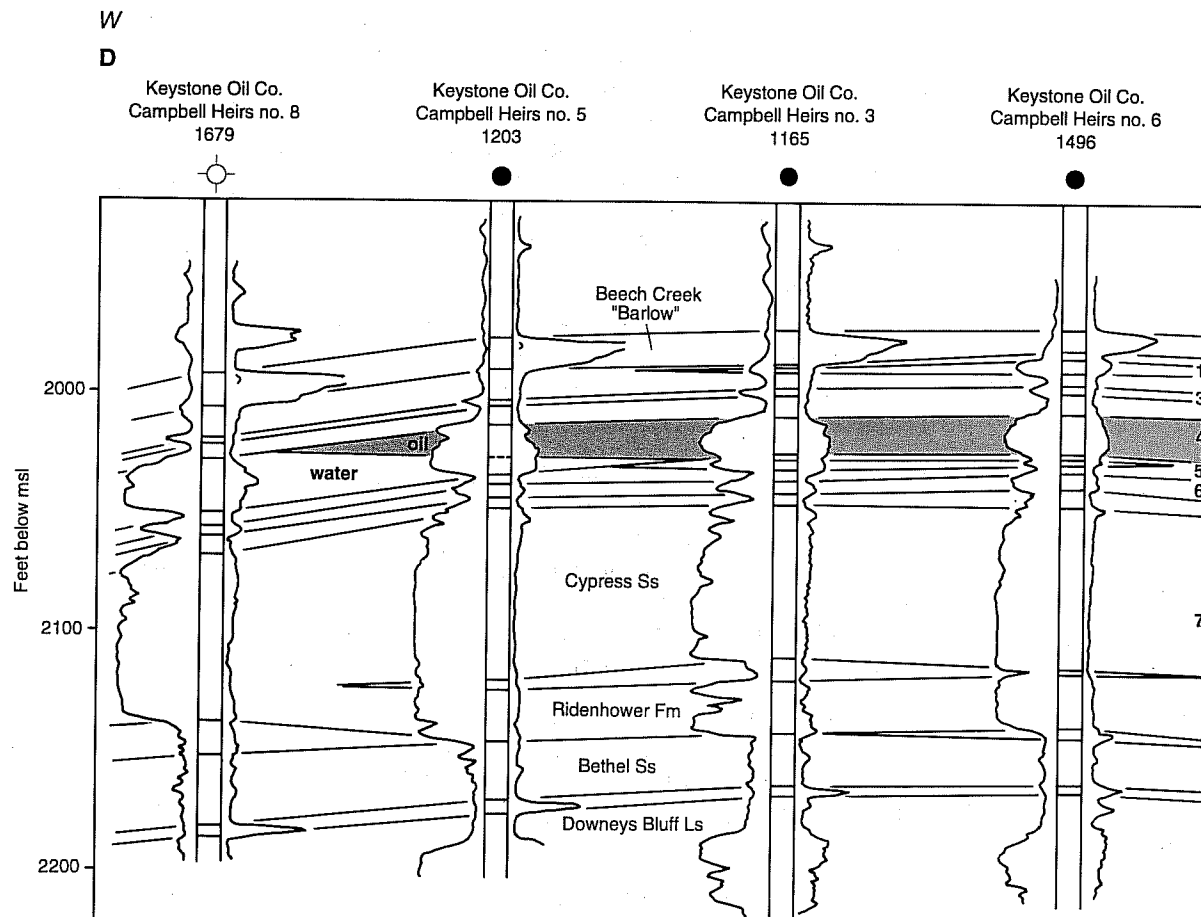
The Cypress Formation in this area is interpreted to have been deposited in environments that ranged from delta front to nearshore and offshore marine. The overlying Barlow limestone establishes a complete depositional cycle from regression to transgression. Other Cypress field studies showing depositional features similar to those observed at Xenia East Field are Bartelso (Whitaker and Finley 1992), Tamaroa (Grube 1992), and Mattoon Fields (McGee, ISGS, personal communication 1992).

Diagenesis

Quartz overgrowths, feldspar dissolution, and authigenic clay mineral formation are the most important diagenetic aspects controlling reservoir quality at Xenia East Field. Other diagenetic features, such as calcite cementation, are not as critical because of their limited distribution.

Quartz overgrowths are the predominant type of cement in the Cypress reservoir. Clastic quartz grains in most samples are enveloped by a layer of secondary quartz growing into a pore until blocked by another grain or overgrowth. These overgrowths are thin or absent in the low permeability part of the reservoir where grains are coated with clay minerals. The grain contacts show little compaction, indicating that quartz overgrowths may have formed early in diagenesis.

Almost all the feldspars in the rocks are altered or dissolved and identification using thin sections is difficult. Results of XRD analyses from Keystone's Campbell Heirs no. 3 show that plagioclase is about twice as abundant as potassium feldspar (fig. 24, table 2). Remnants of partially dissolved feldspar are common around grain-sized voids. Secondary pores formed by feldspar dissolution are illustrated in plates 3 and 4. Molds left by dissolution of feldspar grains are common and apparently have not been affected by compaction. Quartz overgrowths surrounding



some dissolution molds show that feldspar must have dissolved after the major quartz overgrowth event and the end of mechanical compaction.

Kaolinite and iron-rich chlorite are the major diagenetic clay minerals present (plates 4–6). Clay minerals on the surfaces of degraded feldspars and other clastic grains, as well as on the surfaces of quartz overgrowths, indicate that clay minerals formed during a later stage of diagenesis. Although available data are inconclusive, feldspar dissolution most likely provided the elements necessary for the clay minerals to develop.

Table 2 Relative percentages of minerals in core ssamples, as determined by bulk volume (Keystone Oil Company, Campbell Heirs no. 3 well)

County no. /depth (ft)	Relative %				Clay index	Absolute %								
	I	I/S	K	C		I	I/S	K	C	Q	Kf	Pf	Cc	D
1165/2526.5	35.7	11.4	45.5	7.4	0.012	T*	T	0.6	T	92.8	1.5	4.0	T	T
1165/2529.5	30.9	16.2	18.0	34.9	0.026	0.8	T	0.5	0.9	91.6	1.2	4.5	T	T
1165/2533.5	38.5	14.6	20.6	26.3	0.015	0.6	T	T	T	97.3	T	0.8	T	0.0
1165/2535.5	0.0	0.0	79.0	21.0	T	0.0	0.0	T	T	98.0	T	0.9	T	0.8
1165/2540.5	29.7	12.9	39.6	17.8	0.016	0.5	T	0.6	T	90.9	1.9	5.6	0.0	0.0
1165/2542.5	29.4	14.7	43.1	12.9	T	T	T	T	T	95.5	1.0	3.5	T	0.0
1165/2544.5	27.8	7.4	2.6	62.2	0.019	0.5	T	T	1.2	97.1	0.5	T	T	T
1165/2548.8	34.6	10.1	3.9	51.4	0.016	0.5	T	T	0.8	94.5	0.5	3.5	T	0.0

*T = trace, I = illite, S = smectite, K = kaolinite, C = chlorite, Q = quartz, Kf = potassium feldspar, Pf = plagioclase feldspar, Cc = calcite, D = dolomite. Clay index = 4×020 clay peak (19920) + adjusted sum of nonclay peaks.

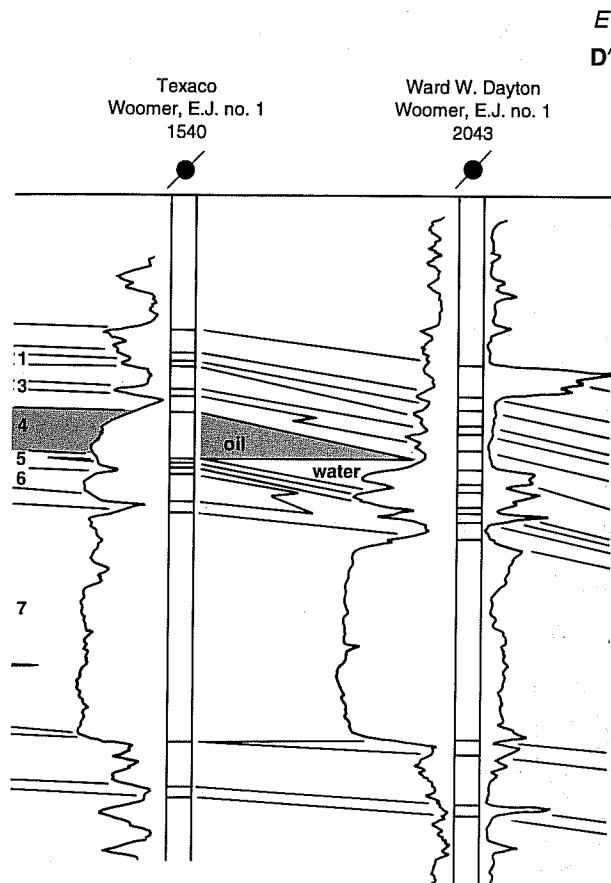


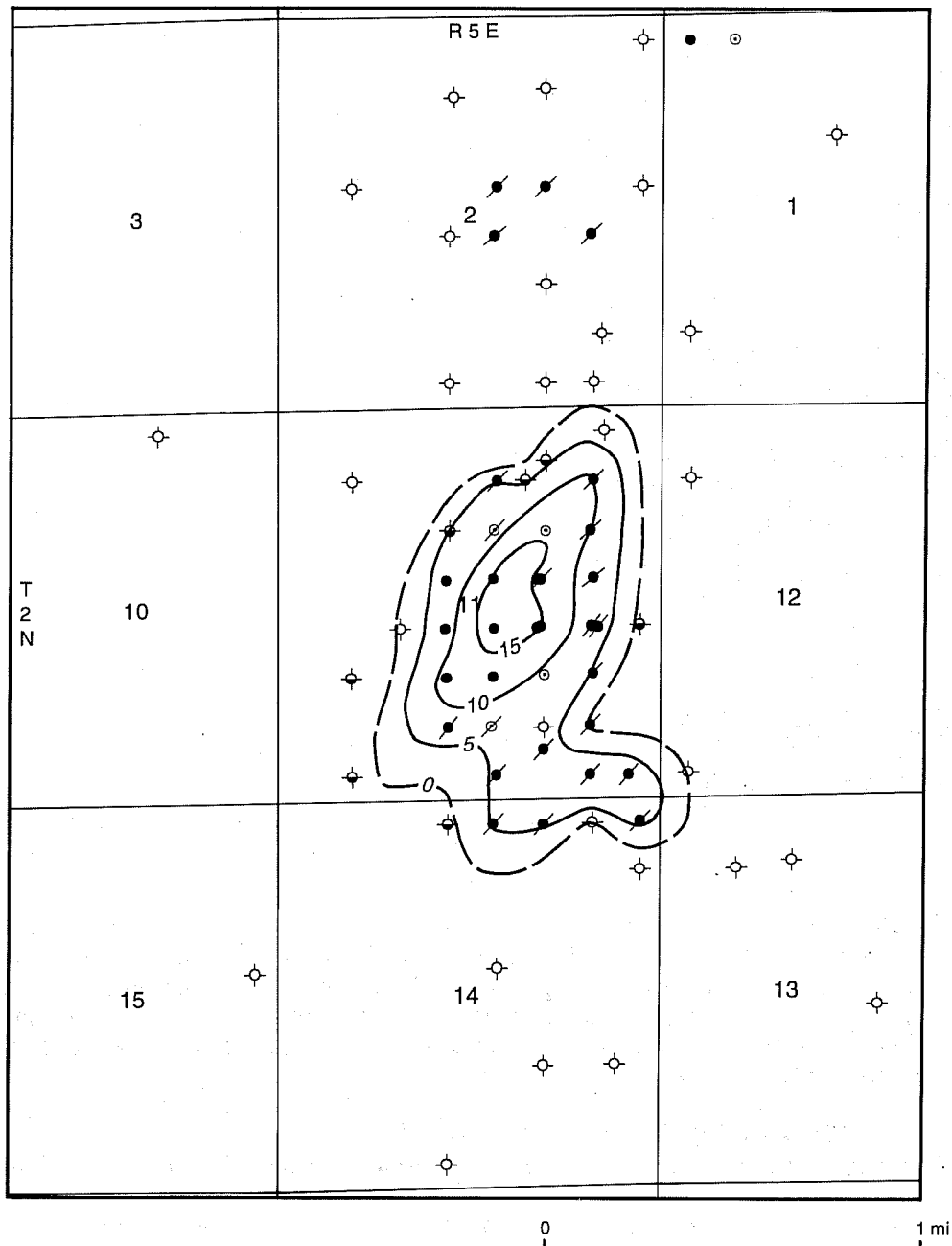
Figure 19 Cross section D-D' (see fig. 15 for location) showing the structural trap in the unit 4 sandstone.

Patchy calcite cement was found in the Cypress Sandstone. All of the calcite cement is iron-rich, as indicated by a potassium ferricyanide stain test. Contact relationships between calcite cement and quartz grains indicate that the patchy calcite may have formed before and/or in the earliest stages of quartz overgrowth. Although it remains a minor component, the amount of calcite cement increases near the top and bottom of the sandstone units.

Factors Controlling Reservoir Quality

Matrix content of the rock and diagenesis are the major factors affecting the reservoir quality. All Cypress wells in the field produce from clean sandstones with little matrix—a facies deposited under relatively high energy conditions. These clean sandstones have higher effective porosity and permeability than dirty sandstones, which were originally low in porosity and permeability because of the presence of clay and silt size matrix. A sample from 2,535.5 feet in Keystone's Campbell Heirs no. 3 well (NW NW SE, Sec. 11, T2N, R5E) has a permeability of 88 md and only a trace (less than 0.5%) of clay, whereas a sample from 2,529.5 feet in the same well has 4.4 md of permeability and approximately 2.6% clay (table 2).

Diagenetic processes that affect reservoir quality include cementation, feldspar dissolution, and formation of diagenetic clay minerals. Quartz overgrowths and calcite precipitation have reduced reservoir porosity, especially the effective porosity. Feldspar dissolution has not only increased secondary porosity, but more importantly, enhanced the permeability. High permeability values always occur in samples with a high number of dissolution pores, although total porosities remain nearly constant throughout the interval. The effect of diagenetic clay minerals on reservoir quality depends upon whether their geochemical environment remains



- | | | |
|-------------------------|-------------------------------|---|
| —— clean sand | ● oil well | ⊙ salt-water disposal converted from oil well |
| - - - oil-water contact | ●/ oil well, plugged | ⊙/ salt-water disposal converted from oil well, plugged |
| | ⊙ oil show, dry and abandoned | |
| | ⊙ dry and abandoned | |

Figure 20 Thickness map of net pay zone, unit 4 sandstone. Contour interval is 5 feet.

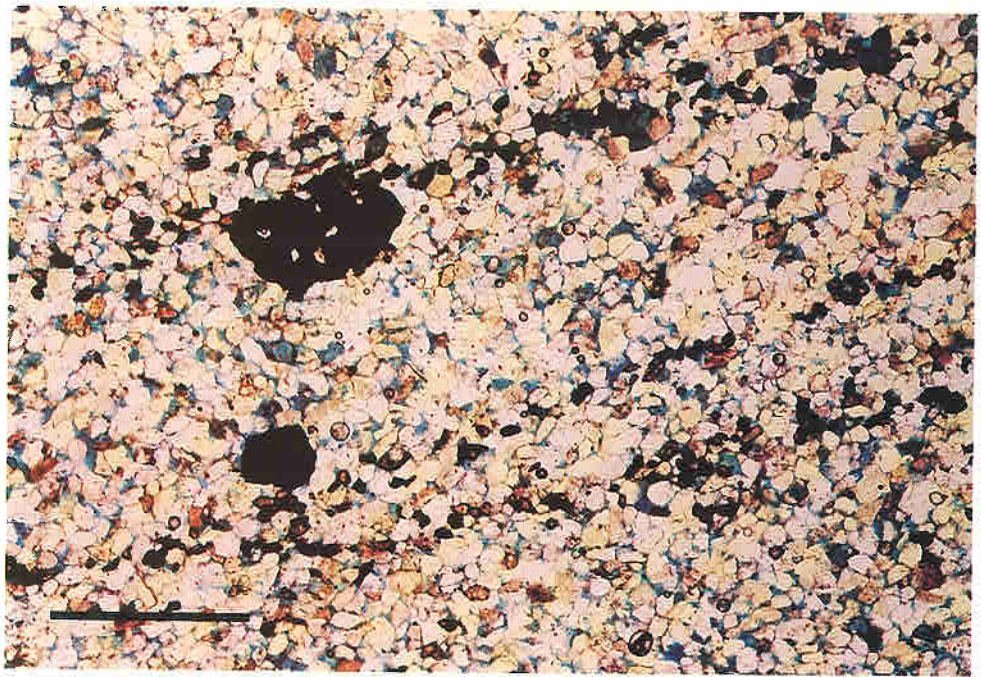


Plate 1 Thin section of a sample from a depth of 2,544.5 feet in the Campbell Heirs no. 3 well. Photomicrograph shows heavy mineral grain lag highlighting the crossbedding in very fine grained sandstone from unit 4. Large black areas are residual oil. Porosity is highlighted in blue. Scale bar is 1 mm.

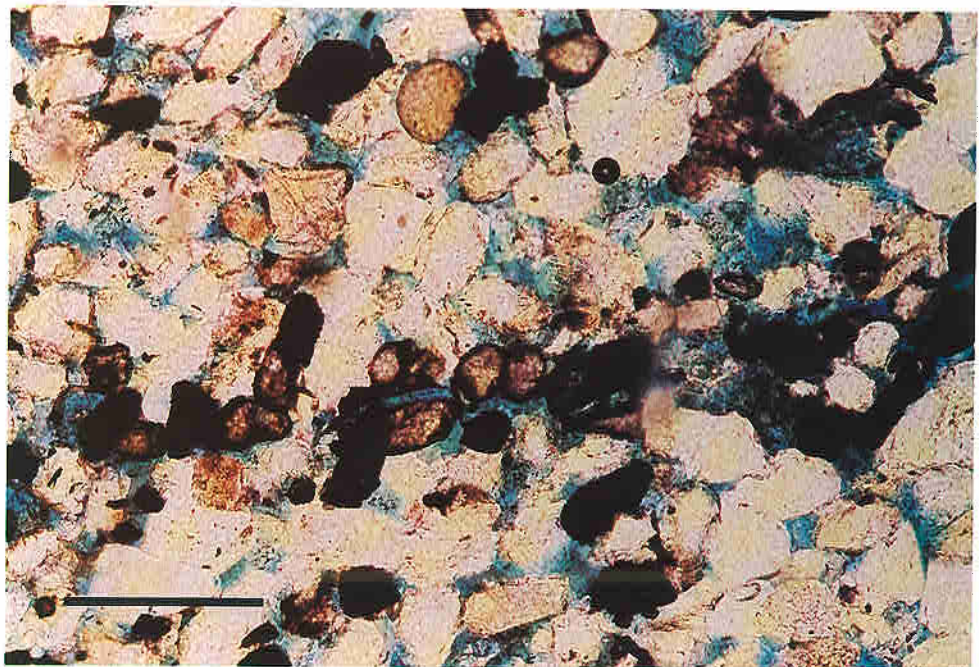


Plate 2 Close-up of the thin section in plate 1. Heavy mineral grains with high optical relief are zircon; black heavy mineral grains are anatase; the brown transparent grain in the upper center of photograph is hornblende. Scale bar is 0.25 mm.

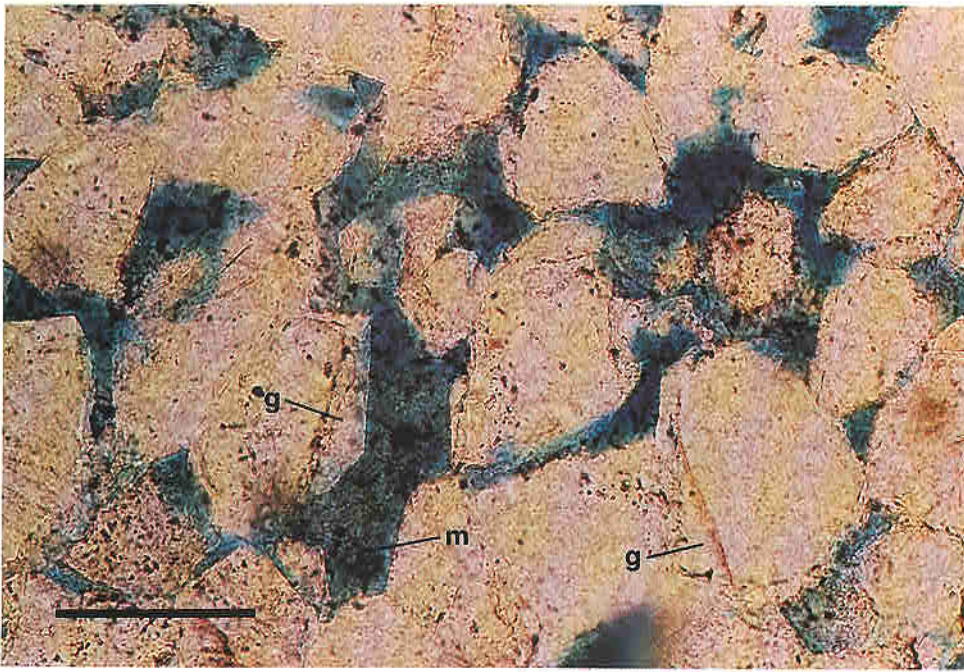


Plate 3 Thin section of a sample from a depth of 2,535.5 feet in the Campbell Heirs no. 3 well. Photomicrograph shows intergranular porosity (blue stain); euhedral, well developed quartz overgrowths (g); and microporosity (m) due to nearly complete dissolution of feldspar grains. Hematite may coat some of the original quartz grains. Scale bar is 0.125 mm.

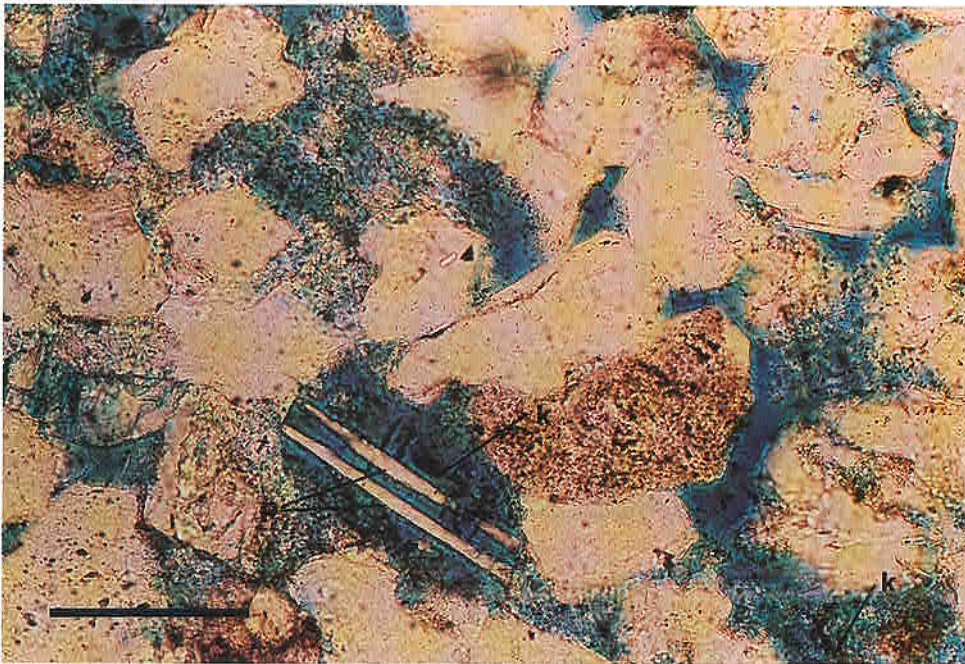


Plate 4 Partially dissolved plagioclase feldspar (p) in the bottom center of the photomicrograph of a thin section of a sample from a depth of 2,536.5 feet in the Campbell Heirs no. 3 well. Two relatively stable albite laths were not dissolved. Large amounts of kaolinite with microporosity (k) are also present. Scale bar is 0.125 mm.

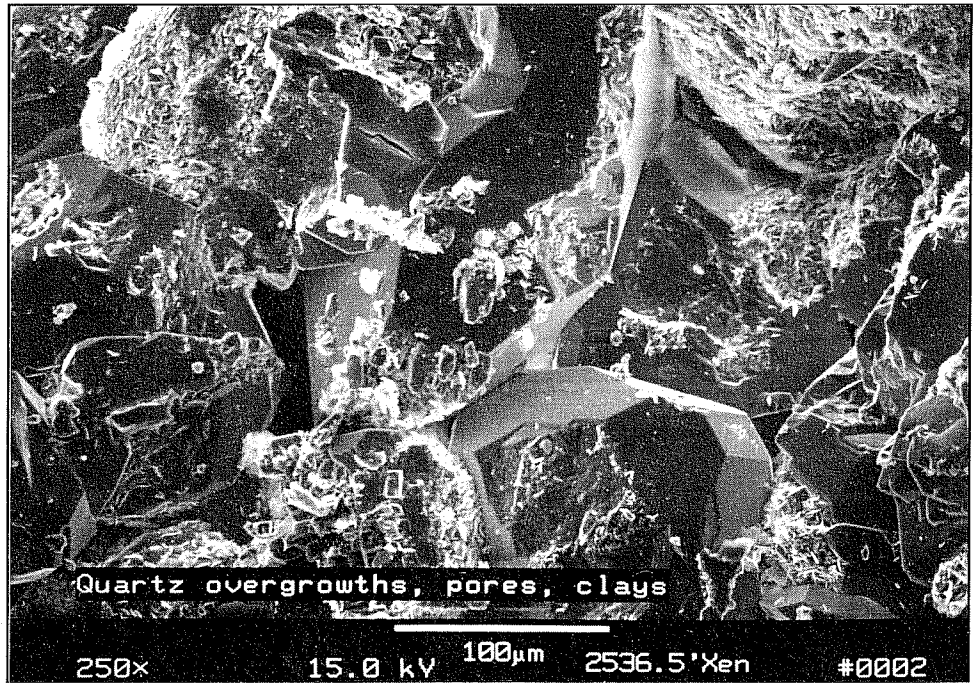


Plate 5 SEM image of a sample from a depth of 2,536.5 feet in the Campbell Heirs no. 3 well shows euhedral quartz overgrowths, pore throats, grain distribution, and precipitation of diagenetic iron-rich chlorite that developed after quartz overgrowths.



Plate 6 SEM image of another area of the sample shown in plate 5 shows dissolution of plagioclase and possible precipitation of albite overgrowths. Diagenetic clay minerals such as chlorite precipitated in pores that developed after the dissolution of feldspars.

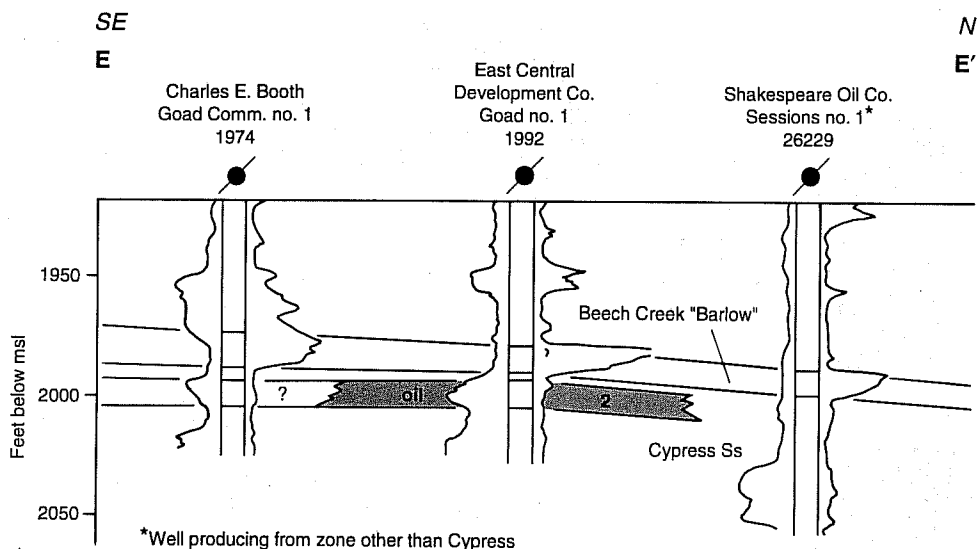


Figure 21 Cross section E-E' (see fig. 17) showing the stratigraphic trap in unit 2 sandstone.

stable. Consequently, the selection of completion and production treatments is critical for preventing reservoir damage.

Quartz overgrowths, which severely reduced primary porosity in most of the clean sandstones, apparently favored the development of secondary porosity. The absence of significant deformation of shale clasts and mica flakes, combined with the absence of sutured quartz grain contacts in the clean sandstones, indicates that early silica cementation in the clean sandstones apparently inhibited mechanical compaction and pressure solution of the sediments. The rigid framework of quartz overgrowths apparently preserved some primary porosity and significant permeability, which otherwise would have been reduced by mechanical compaction. The quartz overgrowths account for the much greater diagenetic alteration and higher permeability in the clean sandstones than in the dirty sandstones. More compaction was observed in the dirty sandstones, where shale clasts and mica flakes are more deformed than they are in the clean sandstones.

Sandstone geometry also affects reservoir quality by inhibiting or diminishing communication of fluids within the sandstone. Vertical permeability barriers and lateral heterogeneities resulting in sandstone compartmentalization apparently were formed by lateral and vertical differences in depositional conditions. Offshore bars, such as units 1 to 3 in the National Association Petroleum Company, Schel Bryan no. 1 well (NE NW SE, Sec. 14, T2N, R5E), are strongly compartmentalized (fig. 7). Examination of SP-logs shows that thin shales sandwiched between sandstone bodies separate the sandstones into compartments. The stratigraphic trap in unit 2 of the East Central Development Company's Goad no. 1 well (SW SE SE, Sec. 11, T2N, R5E) is confined laterally by dirty sandstone. The unit 4 (nearshore bar) reservoir also contains some low permeability intervals (fig. 22), which may be shaly sandstone layers deposited between stacked bars. The shaly intervals do not appear to impede fluid flow because a uniform oil-water contact level was observed for this trap.

CLASSIFICATION AND IDENTIFICATION OF PLAYS

A structurally modified nearshore bar play and a stratigraphic offshore bar play were identified in this field. The structural play has the more significant reserves.

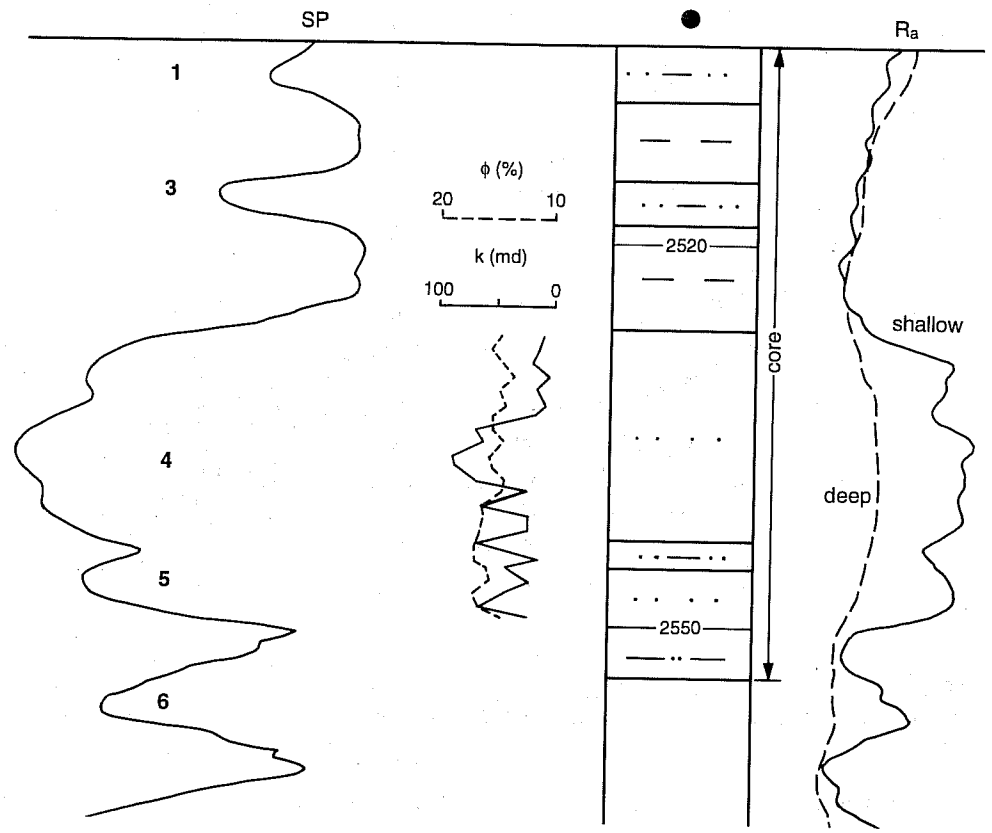


Figure 22 A lithologic column and core analysis combined with an electric log. Porosity (ϕ) and permeability (k) from the core analysis are plotted relative to depth.

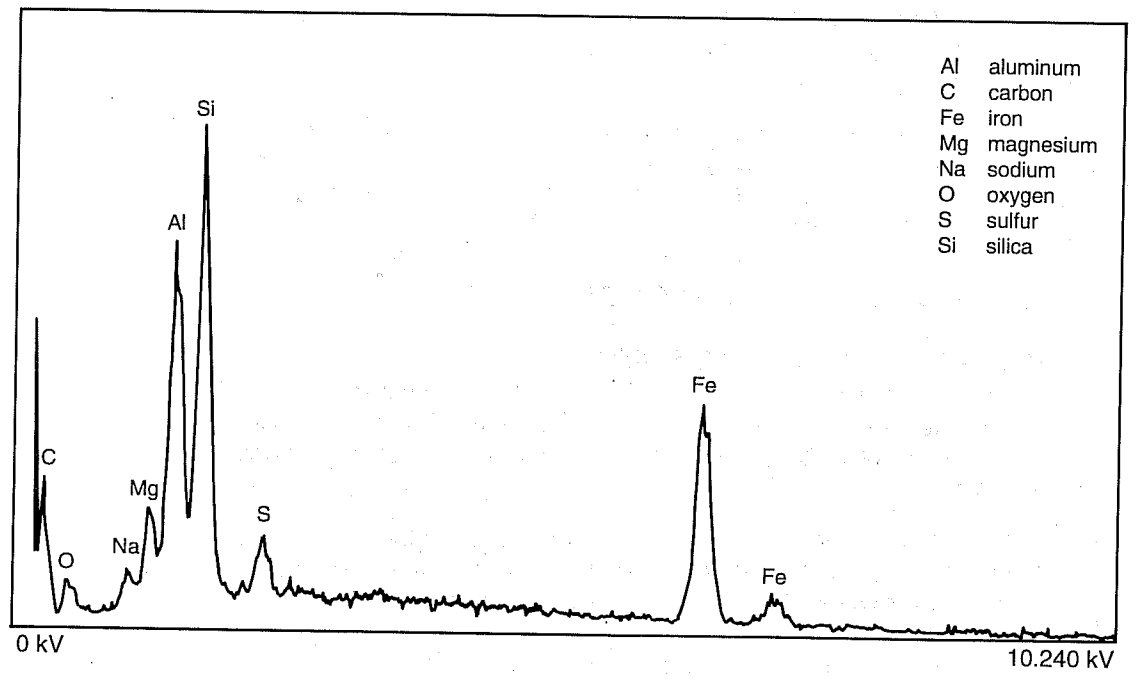


Figure 23 SEM/EDX spectrum of chlorite showing the percentages of elements. The intensity of Fe peaks is especially noticeable.

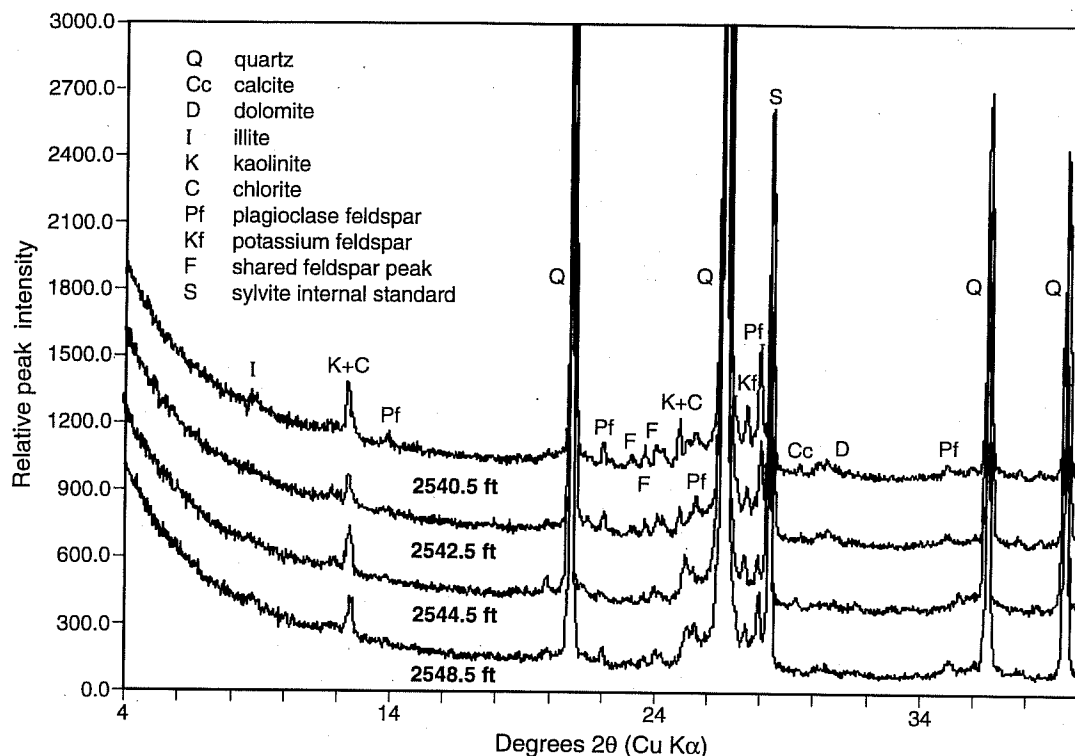


Figure 24 X-ray diffraction results showing the bulk mineral components of the reservoir sandstone. Samples were taken from core plugs of the Campbell Heirs no. 3 well at the depths shown under each spectrum.

The nearshore bar complex consists of sandstone bodies that are usually a few miles long and less than 1 mile wide. Offshore bars consist mainly of thin, dirty sandstones and siltstones, but relatively thick (more than 5 ft) offshore bar sands are also found in the field. An effective trap can be formed in an offshore bar (units 1 to 3) only when the net sandstone is more than 5 feet thick. Because of the sandstone geometry at Xenia East Field, the volume of the offshore trap is smaller than that of the nearshore trap.

Although the lower Cypress Sandstone (unit 7) occurs on the structure at Xenia East, it does not form an effective trap for hydrocarbon accumulation. The failure to trap hydrocarbons may be due to the presence of a strong water drive and the absence of an effective seal.

PRODUCTION CHARACTERISTICS

Drilling and Completion Practices

All wells in the Xenia East Field were drilled with conventional rotary tools. Water-based bentonite mud was used as the drilling fluid in the Cypress productive wells. Most of the wells were completed open hole with casing placed at the top of the reservoir (table 1).

About one-half of the wells were hydraulically fractured at the time of completion. One thousand gallons of lease oil was typically used as the fracturing fluid, and sand was used as a proppant. These treatments yielded fairly good production results (table 1). Primary production was by pump. Initial bottom-hole pressures were as high as 915 psi. The bottom-hole temperature was estimated, on the basis of scout tickets and log header records, to be about 95° F.

Calculation of Reserves

A major objective of this study was to determine the amount of original oil in place (OOIP) and unproduced mobile oil (UMO). The OOIP was calculated by two methods: (1) a volumetric calculation combined with the Monte Carlo technique; and (2) a volumetric calculation based on planimeter measurements. Only the reserves in the major reservoir, the unit 4 sandstone, were calculated. The unit 2 (stratigraphic trap) reserves were not calculated because only one well encountered the trap.

Volumetrics: the Monte Carlo technique The Monte Carlo method is a statistical model that uses random numbers to simulate sampling based on the distribution function(s) of variable(s). Since the 1960s, this method has been widely used to estimate the quantity of petroleum resources (Zhao 1988). The U.S. Geological Survey (USGS) has used the Monte Carlo method for petroleum resource appraisal for the entire United States (Harbaugh et al. 1977, Dolton et al. 1981).

The Monte Carlo method has four distinct advantages for estimating oil resources (Zhao 1988). (1) It can provide not only the estimated amount of the oil resources, but also the degree of uncertainty for the estimated value. (2) It can be applied to any equation for calculating oil resources. (3) It can reduce the bias of a few anomalous datum points because such data will have a small frequency of occurrence in populations with a large sampling. (4) Compared with other statistical methods, it yields a narrower range of reserve estimates, and thus increases the likelihood of a realistic value. Input data include random numbers distributed from 0 to 1, inclusive. Distribution functions of variables are also required. Output from the simulation is a plot of the amount of reserves against their probability of occurrence. Zhao (1988) documents this methodology in detail.

This volumetric equation, as presented in Bradley (1989), was used to calculate the OOIP:

$$\text{Stock tank original oil in place (STOOIP)} = 7,758 \times A \times H \times \phi \times S_o / B_{oi}$$

where

7,758 = conversion factor from acre-feet to barrels

A = reservoir area in acres

H = pay zone thickness in feet

ϕ = average porosity of reservoir sandstone

S_o = oil saturation

The result is the oil volume (bbl) at surface conditions.

For the Monte Carlo estimation, the pay zone thickness and oil saturation were chosen as variables because they have wide ranges; the other parameters in the volumetric equation are constant:

ϕ = 0.153 (averaged from core testing)

A = 416 acres (from grid counting)

B_{oi} = 1.02 (initial oil formation volume factor)

The value of B_{oi} is based on engineering estimates derived from a graphic solution of Standing's correlation (fig. 22.9, p. 22-11, *in* Begg 1987).

Because the populations of H and S_o total less than 30, their distribution functions were built by using an equal frequency method (Zhao 1988); the chance for occurrence of every value is considered to be equal.

The pay zone thickness (H) is based on data from 22 wells. Only 17 wells penetrate the entire producing interval, however, so the pay zone thicknesses for five wells

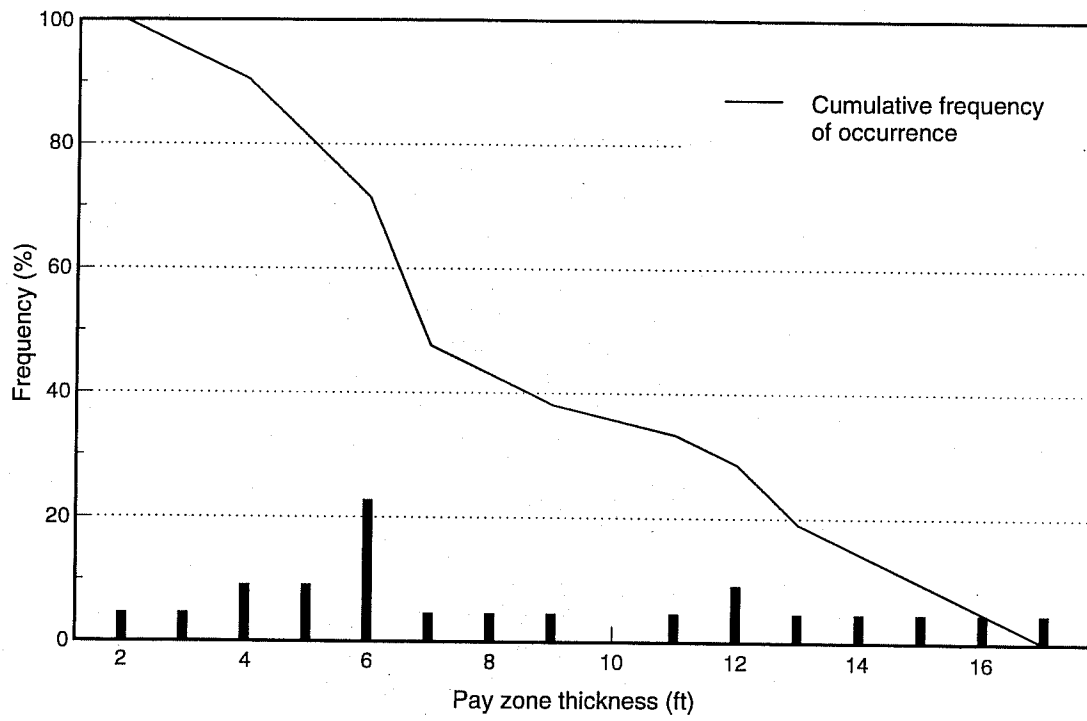


Figure 25 Pay zone distribution function.

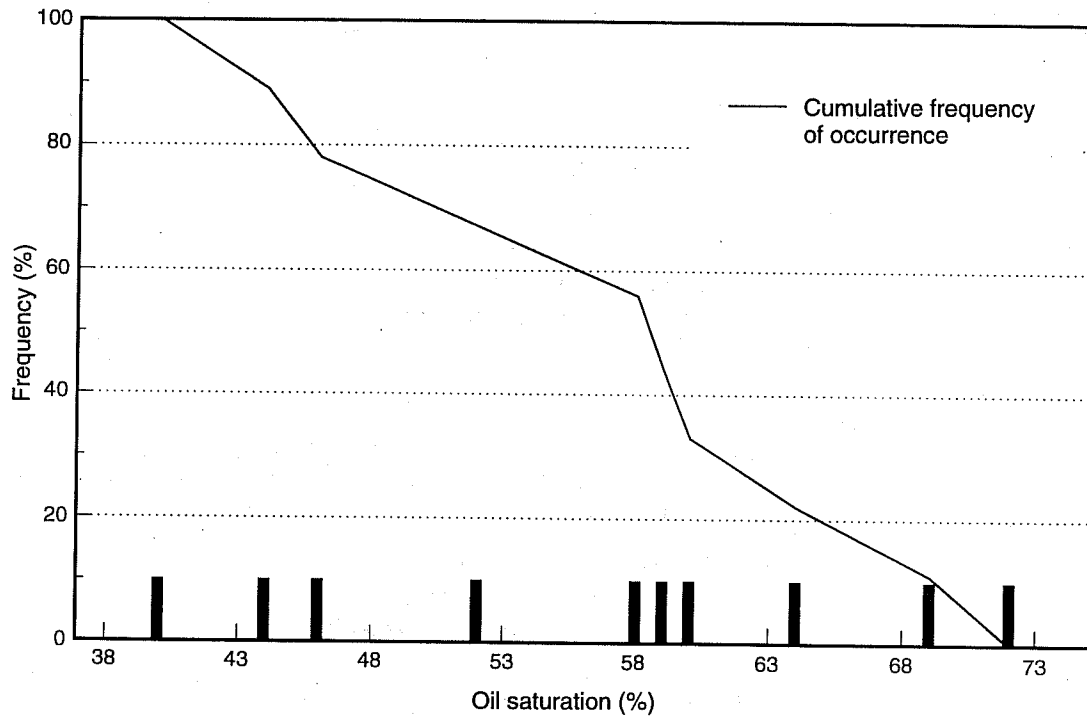


Figure 26 Oil saturation distribution function.

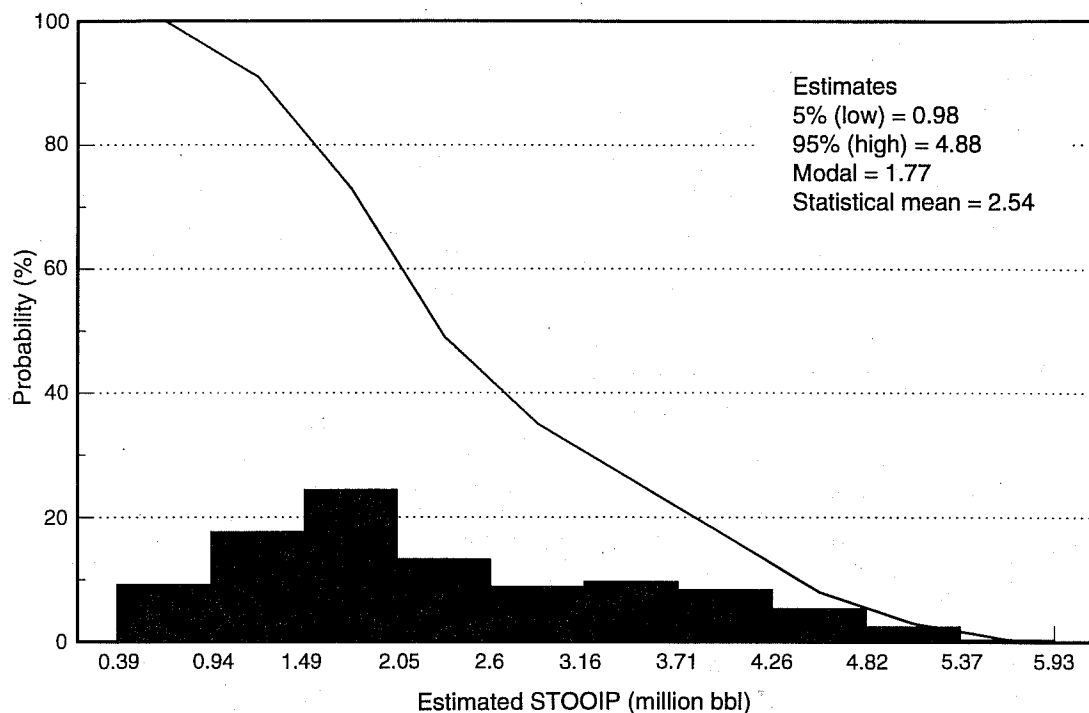


Figure 27 STOPIP distribution function.

were estimated from drilling records and structure maps. Figure 25 shows the distribution function of pay zone thickness. Input data for the function are given in appendix A.

Data on oil saturation (S_o) are not available for the Cypress zones in this field. The S_o data used to construct the distribution function (fig. 26, appendix B) were determined using a Pickett Plot (appendix C). Statistical data for fluvial-dominated deltaic deposits (USDOE 1991) give a range of 41% to 90% for initial oil saturations. Compared with these values, the range for the Xenia East Field is low (40–72%). Data calculated using the Picket Plot are not as accurate as direct measurements, but this is the only way to estimate initial S_o values. When Xenia is compared with other Cypress fields, which have an average S_o of 60%, the results seem consistent.

Monte Carlo calculations were done by direct sampling, using 2,000 random trials on each variable function. The computer program used to generate the calculations is given in appendix B. Because all the geological data are from actual drilling and/or geophysical measurements, their reliability is good and no uncertainty analysis was done for the calculation. The calculated result (probability distribution of STOPIP) is shown in figure 27. Detailed output from the calculation is listed in appendix B.

The method used by USGS geologists (Harbaugh et al. 1979, Dolton et al. 1981) was followed for estimates of STOPIP. A low reserve estimate with a 95% probability is 0.98 million bbl STOPIP (i.e., the probability that the STOPIP was not less than this amount is 95%). A high reserve estimate with a 5% probability is 4.88 million bbl STOPIP (i.e., the probability that the STOPIP in this field exceeded 4.88 million bbl is only 5%). A modal estimate of the STOPIP is 1.77 million bbl, a value associated with the greatest frequency of occurrence among all the estimated reserve intervals. As available data indicate, the modal amount is the one most likely to be present in the field. A statistical mean value for the STOPIP is 2.54 million bbl, calculated by adding the low, high, and modal values and dividing the sum by 3.

The statistical mean estimate lies close to the exact middle of the probability distribution. There is a 45% probability that the STOOIP totaled 2.54 million bbl.

Volumetrics: planimeter measurement The same volumetric equation used for the Monte Carlo calculation was also used to calculate the volumetrics for the field from planimeter measurement of the total reservoir volume. The total reservoir volume ($A \times H$) (using a planimeter-generated measurement of 2,897.7 acre feet [table 3]) was used to calculate a single value of STOOIP, about 2.02 million bbl. Averages of the other variables were used as constants:

$$\begin{aligned}\phi &= 0.153 \\ S_o &= 0.6 \text{ (average Cypress value)} \\ B_{oi} &= 1.02\end{aligned}$$

This estimate is equivalent to the value at the 60% probability on the distribution function of STOOIP generated by the Monte Carlo method (fig. 27).

Discussion of STOOIP and remaining mobile oil Although the Monte Carlo calculation yields a STOOIP range from 0.98 to 4.88 million bbl, the statistical mean estimate of 2.54 million bbl is close to the volumetric estimate of 2.02 million bbl, based on the planimetered measurement. About 451,000 bbl have been produced from the structural trap; these two reserve values (2.54 and 2.02 million bbl) yield primary recovery efficiencies of 18% and 22%, respectively. Other Cypress fields have primary recovery efficiencies of about 20% (Grube 1992, Whitaker and Finley 1992). Because the petrographic characteristics and geological origins of these other fields are similar to those of Xenia East, a similar recovery efficiency could be expected at Xenia East under similar production practices. Therefore, a range of 2.02 to 2.54 million bbl of STOOIP is an acceptable estimate for this structural pool; it corresponds to the 45% to 60% probability range on the STOOIP distribution curve generated by the Monte Carlo method (fig. 27). The amount of producible mobile oil greatly depends on the application of recovery techniques. If operators can increase recovery efficiency to as much as 40% of STOOIP, they can reasonably expect to recover an additional 360,000 to 570,000 bbl of mobile oil from this field. Although the recoverable amount may vary, the remaining reserves (more than 75% of STOOIP) indicate a substantial additional recovery potential.

Table 3 Planimeter measurements

Productive area*	Initial reading	Final reading	Difference	Area** (acres)	Interval H (ft)	Volume [†] (ac-ft)
A ₀	-0.013	1.203	1.216	409.82	-	-
A ₅	-0.011	0.834	0.845	284.78	5	1736.49 ^a
A ₁₀	-0.010	0.254	0.264	88.97	5	888.22 ^b
A ₁₅	-0.010	0.055	0.065	21.91	5	258.38 ^c
A ₁₇	0	0	0	0	2	14.61 ^d
total						2897.7

* A₀ to A₁₇ indicate the areas embodied by the contours of pay zone thickness from 0 to 17 ft, referring to figure 20.

** Correlation factor: 1.899 = 640 acres

[†] The calculations below follow the equations in Craft and Hawkins (1959).

$$^aV = 5/2 (409.82 + 284.78) = 1736.49 \text{ ac-ft}$$

$$^bV = 5/3 [284.78 + 88.97 + (284.78 \times 88.97)^{1/2}] = 888.22 \text{ ac-ft}$$

$$^cV = 5/3 [88.97 + 21.91 + (88.97 \times 21.91)^{1/2}] = 258.38 \text{ ac-ft}$$

$$^dV = 2/3 (21.91) = 14.61 \text{ ac-ft}$$

DEVELOPMENT AND PRODUCTION STRATEGY

Calculations of STOOIP and remaining mobile oil in the Cypress reservoir at Xenia East Field form the basis for recommending secondary recovery techniques such as waterflooding. Primary production has apparently exhausted the original energy in the pool, and waterflooding is a proven method to build and maintain reservoir pressure. Waterfloods have been highly successful in other Cypress fields, including Tamaroa Field in Perry County (Grube 1992) and Bartelso Field in Clinton County (Whitaker and Finley 1992). Because most Cypress production wells have been plugged, new wells may have to be drilled for an effective injection and production program.

Wells producing from formations other than the Cypress at Xenia East are mainly located in the oil-bearing area of the Cypress structural trap (fig. 20). These wells include the Ward W. Dayton, E.M. Goad no. 3 (SW SW NE, Sec. 11, T2N, R5E) and the Keystone Oil Company, Campbell Heirs no. 6 (NE NW SE, Sec. 11, T2N, R5E) and no. 5 (NE NE SW, Sec. 11, T2N, R5E). Perforating the Cypress section in these wells, either to produce oil or inject fluids, would be an efficient short cut and save the expense of drilling new wells.

An overlay of the structure map on the sandstone isopach shows that oil may be trapped in units 5 and 6. Oil shows are reported in drilling logs of these units, so they may hold potentially untapped Cypress reserves. The net sands of the offshore bar sandstones of units 1 to 3 are commonly too thin to form economic reservoirs, even if a trapping mechanism exists.

Drilling and injection fluids must be selected carefully for successful secondary recovery programs in the Xenia East Field. Clay minerals such as kaolinite, mixed-layer illite/smectite, and iron-rich chlorite (table 2) may react with fluids introduced during drilling, completion, and other treatments (Eslinger and Pevear 1988). Leetaru (1991) and Grube (1992) discussed formation damage that can result from the use of fresh water and dilute hydrochloric acid (HCl) in wells. Fluids for field use should be tested in laboratory coreflood experiments to ensure compatibility with the formation. Grube (1992) also found that wells with open hole completions in Cypress Sandstone units at Tamaroa Field showed the highest cumulative production. Because these wells also had higher initial production rates than the cased wells, open hole completions may cause less formation damage and be preferable to perforated completions in Cypress reservoirs.

CONCLUSIONS

The Cypress reservoir in the Xenia East Field consists of sandstone deposited as nearshore and offshore marine bars. Nearshore sandstones, when combined with structural closure, constitute the most important reservoir interval and control almost all the reserves in the Cypress reservoirs. Stacked marine bars form vertically and horizontally heterogeneous reservoirs.

According to estimates made for this study, original oil reserves in this Cypress pool ranged from 2.02 to 2.54 million bbl, and the primary recovery efficiency at Xenia East was about 20% of the STOOIP. Between 360,000 and 570,000 bbl of remaining mobile oil may be producible if a well designed secondary recovery program is implemented. Secondary recovery programs should include infill drilling, perforating Cypress intervals in nonplugged existing wells, waterflooding, and proper completion and treatment procedures.

ACKNOWLEDGMENTS

D.F. Oltz and S.T. Whitaker provided valuable advice and comments during the development and review of this manuscript. We also thank R.D. Cole, J.P. Grube, H.E. Leetaru, K.R. McGee, and E.O. Udegbumam for their useful suggestions. B. Seyler provided the SEM photomicrographs and EDX analyses; D.S. Beaty made the thin sections and performed the XRD analyses.

This report is part of a major research project for reservoir classification and improved and enhanced oil recovery, cofunded by the U.S. Department of Energy (Grant DE-FG22-89BC14250) and the Illinois Department of Energy and Natural Resources (Grant AE-45). Their funding and dedication to the goals of this research are gratefully acknowledged.

REFERENCES

- Armon, W.J., A.A. Coburn, R.F. Mast, and C.W. Sherman, 1964, Physical Properties of Illinois Crude Oil, Part I: Illinois State Geological Survey, Illinois Petroleum 78, p. 52-53.
- Atlas Wireline Services, Illinois Formation Water Resistivity Data: Atlas Wireline Services, Western Atlas International, Inc., unpublished.
- Begg, H.D., 1987 [second printing], Oil system correlations (chapter 22), in H.B. Bradley (editor), Petroleum Engineering Handbook: Society of Petroleum Engineers, Richardson, Texas, p. 22-1 to 22-22.
- Bradley, H.B. (editor), 1989, Petroleum Engineering Handbook: Society of Petroleum Engineers, Dallas, p. 40.1-40.38.
- Craft, B.C., and M.F. Hawkins, 1959, Petroleum Reservoir Engineering: Prentice-Hall, Englewood Cliffs, New Jersey, p. 26-33.
- Davis, R.A., Jr., 1978, Beach and nearshore zone (chapter 5), in Coastal Sedimentary Environments: Springer-Verlag, New York, p. 237-286.
- Dolton, G.L., K.H. Carlson, R.R. Charpentier, A.B. Coury, R.A. Crovelli, S.E. Frezon, A.S. Khan, J.H. Lister, R.H. McMullin, R.S. Pike, R.B. Powers, E.W. Scott, and K.L. Varnes, 1981, Estimates of Undiscovered Recoverable Conventional Resources of Oil and Gas in the United States: U.S. Geological Survey, Circular 860, p. 1-39.
- Dresser Atlas, 1982, Well logging and interpretation techniques, The course for home study: Dresser Industries, p. 38.
- Dresser Industries, Inc., 1979, Pickett cross plot using acoustilog, in Dresser Atlas Open Hole Logging Seminar, unpublished.
- Eslinger, E., and D. Pevear, 1988, Clays and production problems (chapter 8), in Clay Minerals for Petroleum Geologists and Engineers: Society of Economic Paleontologists and Mineralogists, Tulsa, Oklahoma, Short Course Notes 22, 413 p.
- Gerrish, H., 1988, Xenia East Field, in C.W. Zuppann and B.D. Keith (editors), Geology and Petroleum Production of the Illinois Basin, v. 2: Joint Publication of the Illinois and Indiana-Kentucky Geological Societies, p. 193-195.
- Grube, J.P., 1992, Reservoir Characterization and Improved Oil Recovery from Multiple Bar Sandstones, Cypress Formation, Tamaroa and Tamaroa South Fields, Perry County, Illinois: Illinois State Geological Survey, Illinois Petroleum 138, 49 p.

- Harbaugh, J.W., J.H. Doveton, and J.C. Davis, 1977, Probability Method in Oil Exploration: John Wiley and Sons, New York, p. 15–19.
- Hilchie, D.W., 1979, Old electrical log interpretation: IED Exploration, Inc., Tulsa, Oklahoma, p. 43–55.
- Leetaru, H.E., 1990, Application of Old Electric Logs in the Analysis of Aux Vases Sandstone (Mississippian) Reservoirs in Illinois: Illinois State Geological Survey, Illinois Petroleum 134, p. 15–17.
- Leetaru, H.E., 1991, Reservoir Heterogeneity and Improved Oil Recovery of the Aux Vases (Mississippian) Formation at King Field, Jefferson County, Illinois: Illinois State Geological Survey, Illinois Petroleum 135, p. 34–35.
- Meents, W.F., A.H. Bell, O.W. Rees, and W.G. Tilbuty, 1952, Illinois Oil Field Brines—Their Geological Occurrence and Chemical Composition: Illinois State Geological Survey, Illinois Petroleum 66, p. 67.
- Miall, A.D., 1984, Principle of sedimentary basin analysis (chapter 6), *in* Depositional Systems: Springer-Verlag, New York, p. 277–318.
- Moore, D.M., and R.E. Hughes, 1991, Varieties of chlorites and illites and porosity in Mississippian sandstone reservoirs in the Illinois Basin (abstract): American Association of Petroleum Geologists Bulletin, v. 75-3, p. 639.
- Nelson, W.J., 1990, Structural styles of the Illinois Basin, *in* M.W. Leighton, D.R. Kolata, D.F. Oltz, and J.J. Eidel (editors), Interior Cratonic Basins: American Association of Petroleum Geologists, Memoir 51, p. 209–243.
- Petroleum Information, April 1991, Pipeline Production Report: Petroleum Information, Houston, Texas, p. 317.
- Schmidt, V., and D.A. McDonald, 1979, Secondary reservoir porosity in the course of sandstone diagenesis: American Association of Petroleum Geologists, Educational Course Note Series 12.
- Swann, D.H., 1963, Classification of Genevievian and Chesterian (Late Mississippian) Rocks of Illinois: Illinois Geological Survey, Report of Investigation 216, p. 11–17.
- U.S. Department of Energy, 1991, Technical Summary and Proceedings of the Technical Symposium, DOE/BC-91/6/SP, p. 3–30.
- Whitaker, S.T., and Finley A.K., 1992, Reservoir Heterogeneity and the Potential for Improved Recovery within the Cypress Formation at Bartelso Field: Illinois State Geological Survey, Illinois Petroleum 137, 40 p.
- Wichmann, P.A., 1974, Acoustilog, *in* Dresser Atlas, Log Review 1: Dresser Industries, p. 6-1 to 6-13.
- Willman, H.B., E. Atherton, T.C. Buschbach, C. Collinson, J.C. Frye, M.E. Hopkins, J.A. Lineback, and J.A. Simon, 1975, Handbook of Illinois Stratigraphy: Illinois State Geological Survey, Bulletin 95, p. 155.
- Zhao, X., 1988, Petroleum Resource Quantitative Evaluation: Geological Publishing House, China, Chinese edition, p. 42–82.

APPENDIX A Computer Program for the Monte Carlo Calculation

```

INTEGER W, X, Y, Z
CC
CC DIMENSION H(Z), PH(Z), FH(Z)
CC DIMENSION SO(W), PSO(W), FSO(W)
CC DIMENSION Q(Y/2), RH(Y/2), RAND(Y), RSO(Y/2)
CC DIMENSION QIP(X), NQI(X-1), PQI(X-1), APQI(X-1), IQIP(X)
CC
CC W--NUMBER OF OIL SATURATION RECORDS
CC X--THE NUMBER OF POINTS DIVIDING THE INTERVALS OF CALCULATED RESERVES
CC Y--POPULATION OF RANDOM NUMBERS
CC Z--NUMBER OF PAYZONE THICKNESS RECORDS
CC H(Z)--THICKNESS OF PAYZONE
CC FH(Z)--POPULATION OF THE H VALUE IN CORRESPONDING RECORDS
CC PH(Z)--CUMULATIVE FREQUENCY OF OCCURRENCE OF THE H VALUE
CC RH(Y/2)--RANDOM THICKNESS CORRESPONDING THE RANDOM NUMBER
CC SO(W)--OIL SATURATION VALUES
CC PSO(W)--CUMULATIVE FREQUENCY OF OCCURRENCE OF THE SO VALUE
CC FSO(W)--POPULATION OF SO VALUE IN CORRESPONDING RECORDS
CC RSO(Y/2)--RANDOM SO VALUES CORRESPONDING THE RANDOM NUMBER
CC Q(Y/2)--CALCULATED QUANTITY OF RESERVE
CC QIP(X)--Q VALUES DIVIDING RESERVE INTERVALS
CC NQI(X-1)--POPULATION OF Q VALUES IN THE DIVIDED INTERVAL
CC PQI(X-1)--PROBABILITY OF OCCURRENCE OF RESERVE IN DIVIDED INTERVAL
CC APQI(X-1)--CUMULATIVE PROBABILITY OF OCCURRENCE OF THE Q INTERVAL
CC IQIP(X)--INTEGER OF QIP(X)
CC A--AREA OF PAYZONE DISTRIBUTION
CC PO--POROSITY VALUE
CC BOI--OIL VOLUME CONVERSION FACTOR
CC
CC DIMENSION H(15), PH(15), FH(15)
CC DIMENSION SO(10), PSO(10), FSO(10)
CC DIMENSION Q(2000), RH(2000), RSO(2000), RAND(4000)
CC DIMENSION QIP(11), NQI(10), PQI(10), APQI(10), IQIP(11)
CC
CC X=11
CC Y=4000
CC Z=15
CC W=10
CC
CC A=416
CC PO=0.153
CC BOI=1.02
CC CONT=7758
CC
CC INPUT DATA
CC
CC OPEN(1,FILE='HNPHA.',STATUS='OLD')
CC READ(1,*) (H(N),FH(N),PH(N), N=1,Z)
CC
CC OPEN(3,FILE='SONP.',STATUS='OLD')
CC READ(3,*) (SO(M),FSO(M),PSO(M), M=1,W)
CC
CC OPEN(2,FILE='RANDOM.',STATUS='OLD')
CC DO 80 K=1,Y
CC READ(2,*) RAND(K)
80 CONTINUE
CC
CC CALCULATION
CC
CC DO 100 J=1,2000
CC DO 100 I=2, Z
CC IF ((RAND(J) .LT. PH(I-1)) .AND. (RAND(J) .GE. PH(I))) THEN
CC RH(J)=((H(I)-H(I-1))*(RAND(J)-PH(I-1)))/(PH(I)-PH(I-1))
+
CC +H(I-1)
100 CONTINUE

```

APPENDIX A (continued)

```

CC
CC      DO 110 J=2001,Y
          DO 110 I=2,W
              IF ((RAND(J).LT.PSO(I-1)) .AND. (RAND(J) .GE. PSO(I))) THEN
                  RSO(J-2000)=((SO(I)-SO(I-1))*(RAND(J)-PSO(I-1)))/(PSO(I)
+                 -PSO(I-1))+SO(I-1)
                  END IF
110      CONTINUE
CC
CC      DO 120 J=1,2000
          Q(J)=(A*RH(J)*PO*RSO(J)*CONT)/BOI
120      CONTINUE
CC
          HMAX=H(Z)
          HMIN=H(1)
          SOMAX=SO(W)
          SOMIN=SO(1)
          QMAX=(A*HMAX*PO*SOMAX*CONT)/BOI
          QMIN=(A*HMIN*PO*SOMIN*CONT)/BOI
CC
CC      STATISTIC ANALYSIS
CC
          DO 220 J=1, X
              QIP(J)=QMIN+((QMAX-QMIN)/(X-1))*(J-1)
              IQIP(J)=QIP(J)
220      CONTINUE
CC
CC
          DO 250 I=1, X-1
              NQI(I)=0
250      CONTINUE
          DO 300 K=1, 2000
              DO 300 I=2, X
                  IF ((Q(K) .GT. IQIP(I-1)) .AND. (Q(K) .LE. IQIP(I))) THEN
                      NQI(I-1)=NQI(I-1)+1
                  END IF
CC
CC      MAKE UP THE VALUES THAT WERE OMITTED BY INTEGER QIP PROCESS
CC
          IF (Q(K) .GT. IQIP(X)) THEN
              NQI(X-1) = NQI(X-1)+1
          ELSE IF (Q(K).LE.IQIP(1)) THEN
              NQI(1) = NQI(1)+1
          END IF
CC
300      CONTINUE
CC
CC      B=2000
          DO 400 I=1, X-1
              PQI(I)=REAL(NQI(I))/B
400      CONTINUE
CC
CC
          APQI(X-1)=PQI(X-1)
          DO 450 I=X-2, 1, -1
              APQI(I)=APQI(I+1)+PQI(I)
450      CONTINUE
CC
CC      OUTPUT THE RESULT
CC
          OPEN(7, FILE='MTKRESLT', STATUS='NEW')
          WRITE(7,1000) 'INITIAL PETROLEUM RESERVE DATA IN XENIA EAST
+ OILFIELD'
CC

```

APPENDIX A (continued)

```

WRITE(7,1110)
CC
WRITE(7,1010)'PAY ZONE (FT.)','POPULATION OF OCCURRENCE',
+ 'CUMULATIVE FREQUENCY'
CC
DO 500 I=1, Z
WRITE(7, 1020) H(I),FH(I),PH(I)
500 CONTINUE
CC
WRITE(7,1100)
CC
WRITE(7,1010) 'OIL SATURATION', 'POPULATION OF OCCURRENCE',
+ 'CUMULATIVE FREQUENCY'
DO 510 I=1,W
WRITE(7,1020) SO(I), FSO(I), PSO(I)
510 CONTINUE
CC
WRITE(7,1100)
WRITE(7,1090)'FORMULA USED: Q = A*H*PO*SO*7758/BOI'
CC
WRITE(7, 1030) 'HMAX = ', HMAX,
+ 'HMIN = ', HMIN,
+ 'SOMAX = ', SOMAX,
+ 'SOMIN = ', SOMIN,
+ 'QMAX = ', QMAX,
+ 'QMIN = ', QMIN
CC
WRITE(7,1100)
CC
WRITE(7, 1040) 'INTERVAL OF RESERVE (bbls.)', 'PROBABILITY',
+ 'CUMULATIVE PROBABILITY'
CC
DO 600 I=1, X-1
WRITE(7, 1050) IQIP(I), IQIP(I+1), PQI(I), APQI(I)
600 CONTINUE
CC
WRITE(7,1100)
CC
WRITE(7,1080)'OTHER PARAMETERS USED:','A = ',A,'ACRES',
+ 'PO = ',PO,' ','BOI = ',BOI,' (VOLUME FACTOR)'
WRITE(7, 1085) '7758 --',' CONVERSION FACTOR FROM ACRE-FEET
+ TO BARRELS'
CC
WRITE(7, 1110)
WRITE(7, 1070) 'RANDOM', (RAND(N), N=1, Y)
WRITE(7, 1060) 'RANDOM H ', (RH(N), N=1, 2000)
WRITE(7, 1060) 'RANDOM SO', (RSO(N), N=1, 2000)
WRITE(7, 1060) 'RANDOM Q ', (Q(N), N=1, 2000)
CC
1000 FORMAT (1X, 10X, A55)
1010 FORMAT (/,1X, A14, 5X, A30, 5X, A25)
1020 FORMAT (1X, F10.2, 25X, F6.0, 25X, F6.2)
1030 FORMAT (/,1X, 4(A7, F5.2, 6X)/2(1X,A7, F10.2,15X))
1040 FORMAT (/,1X, A27, A16, 8X, A25)
1050 FORMAT (/,1X, I8,1X, '-', I8, 15X, F6.3, 20X, F6.2)
1060 FORMAT (/,1X, A9/6(F11.2, 1X))
1070 FORMAT (/,1X, A6/6(F10.4,2X))
1080 FORMAT (/,1X, A22/(10X,A6,F7.3,A16))
1085 FORMAT (1X, 8X,A7,A44)
1090 FORMAT (/,1X, A40)
1100 FORMAT (/,'-----',
+ '-----')
1110 + FORMAT (2(I),'=====',
+ '=====')
CC
STOP
END

```

APPENDIX B Major Input and Output Data for the Monte Carlo Calculation

Input data

File "HNPHA":*	File "SONP":**
2,1,1	0.40,1,1
3,1,0.95	0.44,1,0.89
4,2,0.90	0.46,1,0.78
5,2,0.81	0.52,1,0.67
6,5,0.71	0.58,1,0.56
7,1,0.48	0.59,1,0.44
8,1,0.43	0.60,1,0.33
9,1,0.38	0.64,1,0.22
11,1,0.33	0.69,1,0.11
12,2,0.29	0.72,1,0

* Each roll of the data is in the order of H(Z), FH(Z), and PH(Z). See definition of the arrays in appendix A.

** Each roll of the data is in the order of SO(X), FO(W), and PSO(W). See definition of the arrays in appendix A.

APPENDIX B (continued)

Output data

Initial petroleum reserve data in Xenia East oil field

Pay zone (ft)	Population of occurrence	Cumulative frequency
2.00	1	1.00
3.00	1	0.95
4.00	2	0.90
5.00	2	0.81
6.00	5	0.71
7.00	1	0.48
8.00	1	0.43
9.00	1	0.38
11.00	1	0.33
12.00	1	0.29
13.00	1	0.19
14.00	1	0.14
15.00	1	0.10
16.00	1	0.05
17.00	1	0.00

$$\text{Formula used: } Q = \frac{A \times H \times \phi \times S_o \times 7,758}{B_{oi}}$$

where

$$\begin{aligned} A &= 416.000 \text{ acres} \\ B_{oi} &= 1.020 \text{ (volume factor)} \\ \phi &= 0.153 \\ H_{\max} &= 17.00 \\ H_{\min} &= 2.00 \\ S_{o \max} &= 0.72 \\ S_{o \min} &= 0.40 \\ Q_{\max} &= 5925374.50 \\ Q_{\min} &= 387279.34 \\ 7,758 &= \text{conversion factor from} \\ &\quad \text{acre-feet to barrels} \end{aligned}$$

Oil saturation	Population of occurrence	Cumulative frequency
0.40	1	1.00
0.44	1	0.89
0.46	1	0.78
0.52	1	0.67
0.58	1	0.56
0.59	1	0.44
0.60	1	0.33
0.64	1	0.22
0.69	1	0.11
0.72	1	0.00

Reserve range (bbl)	Probability	Cumulative probability
387279– 941088	0.092	1.00
941088–1494898	0.177	0.91
1494898–2048707	0.244	0.73
2048707–2602517	0.133	0.49
2602517–3156326	0.089	0.35
3156326–3710136	0.097	0.26
3710136–4263946	0.084	0.17
4263946–4817755	0.054	0.08
4817755–5371565	0.025	0.03
5371565–5925374	0.004	0.00

APPENDIX C Pickett Plot Data

The Pickett Plot method plots porosity versus resistivity of the formation (R_t) on log-log paper from which the S_w/S_o values of the samples are derived.

Long normal (R64") and short normal (R16") E-logs were used to determine R_t in this study. Because of the bed thickness requirement, only 14 wells in the production area could be used for this application; the results for 12 wells were reasonable, based on derived values versus test data (fig. C-1). Bed thickness and adjacent bed resistivity corrections have been applied to both the long and short normal readings. Invasion effects were corrected using Hilchie's (1979) empirical relationship:

$$R_t = (R_{64} \times R_{16}) / R_{16}$$

An average porosity of 15.3%, calculated from a core analysis from the Campbell Lease no. 3 (fig. 23), was used in the plot.

The resistivity of water in rock, $R_w = 0.046$ ohm-m (Atlas Wireline Services, unpublished), was used to construct the 100% S_w line. A 1.88 ohm-m value based on log interpretation was chosen as R_o , the resistivity of 100% water-bearing rock. The reversed slope of the 100% S_w line defined by these two points is about 2, coinciding with the range of m (rock cementation factor, 1.8 to 2.2 in most sandstones [Dresser Atlas 1982]). Additional water saturation lines on this graph were determined by different R_t/R_o ratios (Dresser Industries 1979, Wichmann 1974, Leetaru 1990). The plot result is shown in figure C-1. S_o values (fig. 27 and appendix B) were estimated by interpolation.

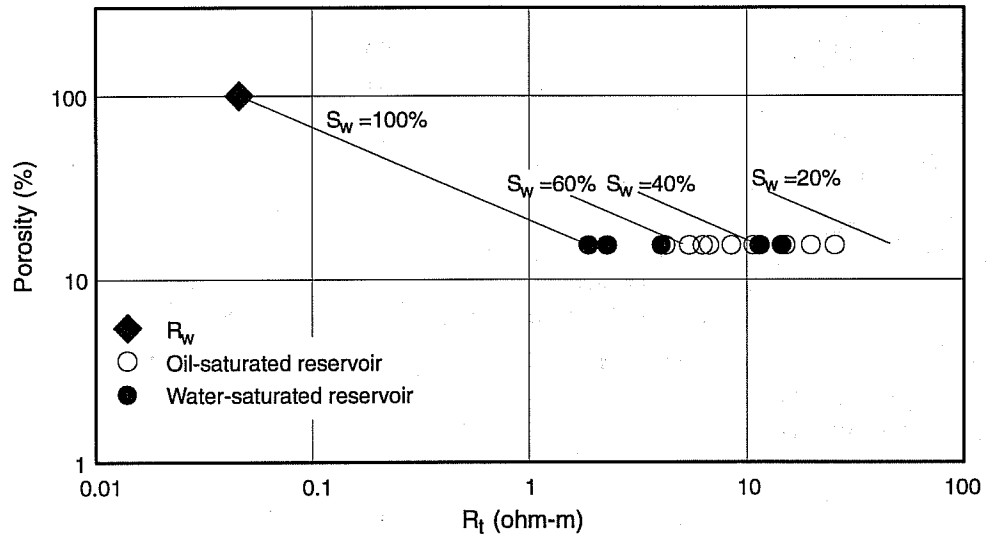


Figure C-1 Pickett Plot showing the initial water-oil saturations of the reservoir.

APPENDIX D Reservoir Summary

Field Xenia East

Location Clay County, Illinois; Sections 11 and 14, T2N, R5E

Tectonic/Regional Setting intracratonic basin

Geologic Structure anticline

Trap Type structural and stratigraphic

Reservoir Drive water drive

Original Reservoir Pressure NA; DST shut-in BHPs as high as 915 psi

Reservoir Rocks

Age Mississippian (Chesterian)

Stratigraphic unit Cypress

Lithology quartz arenite

Wetting characteristics NA

Depositional environments nearshore and offshore marine bars, vertically stacked

Productive facies sandstones of the central bar

Petrophysics (ϕ and k from unstressed conventional core; S_w from E-log interpretation)

Porosity type (ϕ total = average 15.3%, primary 13.3%, secondary 2%)

	Average	Range	Cutoff
ϕ (%)	15.3	13.5–17	13.5
k air (md)	71	4–88	NA
k liquid (md)	NA	NA	NA
S_w (%)	40	60–28	60
S_{or} (%)	NA	NA	NA
S_{gr} (%)	NA	NA	NA
Cementation factor	NA	NA	NA

Source Rocks

Lithology and stratigraphic unit NA

Time of hydrocarbon maturation NA

Time of trap formation Chesterian (stratigraphic); NA (structural)

Cypress Reservoir Dimensions

Depth 2,480 to 2,540 ft

Areal dimensions 10 acres

Productive area 285 acres

Number of pay zones 2

Hydrocarbon column structural 17 ft, stratigraphic 9 ft

Initial fluid contacts structural oil/water = -2,030 ft; stratigraphic none

Ave. net sand thickness unit 4 = 15 ft, unit 2 = 5 ft

Ave. gross sand thickness unit 4 = 17 ft, unit 2 = 9 ft

Net/gross unit 4 = 0.9, unit 2 = 0.6

Initial reservoir temperature as high as 100°F (from log header)

Fractured natural unknown; artificial = lease oil-sand induced

Appendix D (continued)

Wells

Spacing 10 acre primary

Pattern normal primary

Total

Cypress producers 18 originally (17 in structural trap, 1 in stratigraphic trap); 4 disposal; 17 abandoned, recorded; 21 dry holes; 0 water source, observation; 0 suspended; 0 injection; 12 producers from other formations

Reservoir Fluid Properties

Hydrocarbons^(a)

Type oil

GOR NA

API gravity 37.2

FVF 1.02 (estimated)

Viscosity 4.44 Cp @ 100°F, 6.10 Cp @ 77°F, 12.88 Cp @ 50°F

Bubble-point pressure NA

Formation water

Resistivity 0.046 @ 100°F^(b)

Total dissolved solids 126,700 to 128,380 PPM^(c)

Volumetrics

In-place

Structural 2.02–2.54 million bbl STOOIP

Stratigraphic NA

Cumulative production total 470,000 bbl, 451,000 from structural trap and 19,000 from stratigraphic

Ultimate recovery

Primary 470,000 bbl

Secondary no secondary recovery projects attempted to date. A possibility of 360,000 to 570,000 bbl of oil may be recovered

Recovery efficiency

Primary approximately 18–22% for the structural

Secondary unknown

Typical Drilling/Completion/Production Practices

Completions open hole or cased

Drilling fluid fresh-water mud with gel additive

Fracture treatment 1000-gallon lease oil with sand combination

Acidization none

Producing mechanism pump

Typical Well Production (to date)

Average daily IP 56 BOPD; range 8 to 152 BOPD

Cumulative production 26,100 bbl (primary); range NA

Water/oil ratio (initial) 0.7; range 0 to 4